Enhanced Resiliency in Corporate Bond Liquidity: A Tradeoff in OTC Markets *

Botao Wu
CUHK

This draft: November 2025
First draft: February 2025

Abstract

I argue that post-financial crisis regulations created a fundamental tradeoff between immediacy and resiliency in corporate bond market liquidity. While existing studies have documented that stricter capital requirements reduced dealer inventories and lengthened trading delays in normal times, this paper highlights the intended benefits of these regulations: enhanced market resiliency during crises. Using data from the Great Financial Crisis (GFC) of 2008 and the COVID-19 pandemic of 2020, I show that the corporate bond market recovered from systemic shocks significantly faster in the post-GFC era. This improved resiliency stems from a behavioral shift among better-capitalized dealers, who, unlike in the GFC, were able to "lean against the wind" by absorbing systemic selling pressure. This effect is most pronounced for high-yield bonds, which experienced the largest regulatory-induced declines in normal-time immediacy but, in turn, exhibited the most significant gains in crisis-time resiliency. I develop a stylized over-the-counter (OTC) model that formalizes this immediacy-resiliency tradeoff and provide a balanced framework for assessing the welfare implications of post-GFC regulations on market liquidity.

Keywords: Corporate Bond Liquidity, Resiliency, Regulations, Welfare, Financial Stability

JEL classification: G10, G12, G18, G20

*Contact: botaowu@cuhk.edu.hk. I appreciate conversations with Farshid Abdi, Vladimir Atanasov, Jaewon Choi, Peter Feldhütter, Joel Hasbrouck, Benjamin Lester, Maureen O'Hara, Matthew Pritsker, Chaojun Wang, and participants at EFA 2025 Paris, FMA 2025, CUHK Junior workshop, and the IOSCO/OECD Conference on Corporate Bond Markets. I am grateful to the research support by the Early Career Scheme from the Hong Kong SAR government.

1 Introduction

Corporate bond market liquidity has been a subject of heated debate since the great financial crisis (GFC). Post-GFC banking regulations introduced stricter capital requirements for dealer banks. It is well documented that these regulations have introduced unintended costs for corporate bond market liquidity, as they stipulate stringent limits on the amount of dealer capital that can be committed to trading during normal times. These regulations therefore reduce dealer banks' inventory holdings and their provision of immediacy during normal times. Investors now need to spend more time waiting to fully execute their trades.[1]

While the initial, acute phase of the COVID-19 crisis in March 2020 saw severe market dislocations, I argue that the right angle to assess the market's structural health is through its resiliency—namely, how quickly prices can recover from a systemic liquidity shock. When a shock creates one-sided selling pressure, it is natural for prices to fall and bid-ask spreads to rise. What truly matters for financial stability is how long this disruption lasts and how deep the price crash becomes. From this perspective, I show that the resilience of corporate bond liquidity has actually improved dramatically in the post-GFC era. Post-GFC regulations made dealer banks better capitalized. They were no longer forced to de-risk and sell into a falling market as they did during the GFC. Instead, better-capitalized dealers were able to "lean against the wind," absorbing the strong selling pressure, thereby stabilizing prices and contributing to a faster recovery. Such improved resiliency, I argue, is one of the intended benefits of post-GFC regulations on OTC market liquidity.

I document this improved resiliency by measuring the dynamic response of credit spreads to a systemic liquidity shock, proxied by the VIX. These impulse responses capture both the elevation in credit spreads in response to a liquidity shock as well as the time duration for the credit spread to fully absorb the liquidity shock. I find that while it used to take more than 15 weeks for liquidity shocks to be fully absorbed by credit spreads before the GFC, this absorption is now far more rapid. The half-life of a liquidity shock's impact on credit spreads plummeted from over 21 weeks during the 2001-2009 period to just under 7 weeks in the 2012-2020 period. Alternative measures,

[1] Goldman Sachs Global Investment Research: *"it isn't that they can't get trades done; it's that they can't get trades done as quickly [...] [T]rade that historically may have taken a day to get done now needs to [...] take a week or two to execute."* Source: https://www.goldmansachs.com/insights/pages/macroeconomic-insights-folder/liquidy-top-of-mind/pdf.pdf.

such as the price impact of order flows or the mean-reversion rate of yields, all point to the same conclusion: a substantially more resilient corporate bond market in the post-GFC era.

The mechanism behind this greater resiliency is a fundamental shift in dealer behavior, enabled by a change in their balance sheet structure. I document that during the GFC, dealers acted pro-cyclically, dumping bonds and exacerbating market instability. In sharp contrast, during the COVID-19 pandemic, dealers acted counter-cyclically, increasing their corporate bond holdings in response to the liquidity shock. This "leaning against the wind" behavior is not merely a choice but a direct consequence of the regulatory environment. Rules like the Stressed Value-at-Risk (SVaR) constraint forced dealers to hold less inventory in normal times by requiring them to capitalize against a stressed scenario. This regulatory-induced reduction in normal-time inventory created the very "spare" balance sheet capacity that enabled them to absorb selling pressure when a real crisis hit, contributing to a faster recovery of the market.

To identify the role of regulation, I separate the sample into investment grade bonds and speculative high-yield bonds. As high-yield bonds are most penalized by capital regulations in normal times, it is therefore not surprising to find that the improvement in resiliency is concentrated in the high-yield bond market due to the same regulations. The credit spread response to liquidity shocks has only been reduced substantially for high yield bonds, while for the highly rated investment grade bonds the credit spread response to liquidity shocks has remained the same. Furthermore, I show that while dealers were net sellers of both investment-grade and high-yield bonds during the GFC, they became significant net buyers of high-yield bonds during the COVID-19 crisis. Finally, I provide direct evidence that this improvement in resiliency is driven by the largest and most regulated dealers: whereas they heavily reduced inventory during the GFC, they experienced far milder initial dip compared to the smaller, non-regulated dealers during the onset of the COVID-19 crisis and acted counter-cyclically by absorbing assets and stabilizing the market subsequently. This effect was absent during the GFC, when bonds traded by both regulated and non-regulated dealers suffered from a similar lack of resiliency.

To rationalize these empirical findings, I build a stylized OTC market in the spirit of Lagos and Rocheteau (2007), augmented with two aggregate states of the economy: normal times and crisis times. One novelty of the model is that I link regulations to the liquidity of the OTC market via

the dealer inventory (I) and total balance sheet capacity ($\bar{I}$). In normal times regulations reduce the dealer inventory I, delaying the search time between the customers and dealers and therefore harming the immediacy dimension of the OTC liquidity. In times of crisis, this lower inventory implies greater spare capacity ($\bar{I} - I$) for dealers, which accelerates the market's recovery from the crisis. This central mechanism is not merely a stylized assumption; it can be formally microfounded by imposing a Stressed Value-at-Risk (SVaR) constraint on dealers. The model thus formalizes this immediacy-resiliency tradeoff in the OTC market, and is able to generate rising trading delays and liquidity premium in normal times but smaller price crashes and faster recoveries in crisis times when dealer inventory is reduced, all of which are consistent with the empirical patterns documented in the literature.

One key advantage of the model is that it allows for a welfare analysis of post-GFC regulations on the OTC market liquidity. Existing studies, by focusing only on the costs to immediacy, would imply an optimal inventory level of 100% of the total capacity. In my framework, however, using full capacity in normal times is actually suboptimal, as it leaves dealers no spare capacity for a crisis and makes the market extremely fragile. I derive an analytical welfare function that balances the costs of reduced immediacy in normal times against the benefits of enhanced resiliency in crisis times. A calibration exercise, disciplined by my empirical findings, suggests an optimal dealer inventory level of approximately 20% of total capacity, a figure strikingly consistent with the observed reduction in dealer inventories in the post-GFC era.

This paper contributes to the following strands of literature. First, this is one of the first papers to document the improved resiliency in corporate bond liquidity after the great financial crisis. Doing so I complement Becker and Benmelech (2021) who show that bond issuance is more resilient than loan issuance in a crisis. My results suggest that the faster recovery for corporate bond yields to absorb liquidity shocks may help encourage bond issuance in times of crisis. O'Hara, Rapp, and Zhou (2021) show that insurance companies help support the resilience of investment grade bonds during the COVID crisis. I complement their work by showing that high-yield bonds have also enjoyed improvement in the resiliency and better capitalized dealers are more likely to be the main contributors because insurance companies do not own high-yield bonds due to their investment mandates. More broadly, my paper provides a new perspective on the corporate bond

market's performance during the COVID-19 crisis. A series of influential papers have documented the severe, acute deterioration in liquidity during the peak panic of early March 2020, showing that dealers initially pulled back from the market (e.g., Kargar et al. 2021, O'Hara and Zhou 2021), and that the Federal Reserve's subsequent announcements were critical for restoring market functioning (e.g., Boyarchenko, Kovner, and Shachar 2022; Gilchrist et al. 2024). My analysis complements their work by taking a longer, comparative view. My focus is on the market's subsequent resiliency and its contrast with the prolonged dysfunction of the 2008 GFC period. My findings suggest that post-GFC regulation, by creating more robust dealer balance sheets, enabled a faster and more resilient recovery once the Federal Reserve's decisive actions had quelled the initial panic. This insight motivates me to run a formal counterfactual analysis that uses the model to quantify how the Fed's 2020 intervention would have performed in a pre-GFC regulatory environment. The results suggest that the very same intervention would have been nearly half as effective in the pre-GFC period, resulting in a significantly deeper price crash and a recovery time almost twice as long. This demonstrates a crucial yet previously unquantified complementarity: post-GFC regulations created a market structure that amplified the power of the central bank's crisis-fighting toolkit.

Second, my paper offers a more comprehensive assessment of post-GFC regulations on bond liquidity. It reconciles the well-documented costs of reduced immediacy (e.g., Dick-Nielsen and Rossi (2018), Bao, O'Hara, and Zhou (2018), Bessembinder et al. (2018)) with the previously under-appreciated benefits of enhanced resiliency. It should be noted that I am not arguing against the existing conclusions of the worsened immediacy due to regulations such as the Volcker rule. Instead, I am pointing out such loss of immediacy is the necessary cost for a more stable system, a goal that regulators have intended in the first place. My paper highlights the importance of flexible, state-contingent regulation that requires regulators to relax the capital requirement whenever necessary. When regulators fail to do so, we end up in the worst of both worlds: a worsened immediacy in normal times and a lack of resiliency in times of crisis, which should be the true concerns shared by regulators and practitioners. The tradeoff between immediacy and resiliency is also in part supported by the empirical findings in U.S. treasury market. Duffie et al. (2023), and He, Nagel, and Song (2022) observe that regulations have made the treasury market less resilient during the COVID crisis. The impact of regulations on the treasury market can be seen as the exact opposite

of what happens to the corporate bond market: dealers' treasury inventory has actually increased in normal times after the great financial crisis (Adrian et al. 2017, Du, Hébert, and Li 2023), shrinking the balance sheet capacity for crisis times and resulting in elevated treasury yields and disruptions during the pandemic.

Finally, my paper contributes to the literature on OTC search models following Duffie, Gârleanu, and Pedersen (2005), including some more recent works that feature dealer inventory (e.g., Hugonnier, Lester, and Weill 2019, Cohen et al. 2024). Broadly speaking, two types of such models exist. Duffie, Gârleanu, and Pedersen (2005) and Lagos and Rocheteau (2009) study the steady states and show that slower trading speed reduces an asset's value relative to its fundamental. Weill (2007) and Lagos, Rocheteau, and Weill (2011) study the transitional dynamics and characterize price crashes and recovery in response to an aggregate liquidity shock. By introducing two aggregate states, my model is one of the first to formally link the immediacy and resiliency strands of this literature via a single mechanism: dealer inventory and balance sheet capacity. This framework suggests that the transition intensity out of a crisis, the recovery speed, is a first-order parameter for understanding resiliency. Using the empirically estimated half-life of liquidity shocks from my impulse response analysis, I introduce a novel method for calibrating this key resiliency parameter. Doing so I complement recent works that use empirical data to better discipline the calibration of these theoretical models (e.g., Wu 2020, Kargar et al. 2024).

The rest of the paper is organized as follows. In Section 2 I outline an OTC model that features the tradeoff between the immediacy in normal times and resiliency in crisis times. In Section 3 I empirically document the improvement in the resiliency dimension of corporate bond liquidity and link it to regulation. In Section 4 I use my model to conduct a welfare analysis of the post-GFC regulations on corporate bond liquidity. Section 5 concludes.

2 An OTC Model of Immediacy vs. Resiliency

To formalize the tradeoff between the immediacy and resiliency dimensions of liquidity, I develop a stylized OTC model in the spirit of Lagos and Rocheteau (2007) and Lagos, Rocheteau, and Weill (2011), augmented with aggregate state transitions. The economy features a fixed supply A of a

single bond and is populated by two types of customers, High (H) and Low (L), who differ in their valuation of the bond ($\epsilon_H > \epsilon_L$). Customers are subject to idiosyncratic preference shocks arriving at a Poisson rate δ. The key feature of this model is the presence of two aggregate states: a Normal state (N) and a Crisis state (C). The economy switches from N to C at a rate λ^N and recovers from C to N at a rate λ^C. In the Normal state, aggregate valuation is high (z^N), while in the Crisis state, it is low ($z^C < z^N$). Customers trade with dealers in a search market, meeting them at a Poisson rate α.

Consider a stochastic stationary equilibrium. The value function of customer $i \in \{H, L\}$ in the aggregate state $s \in \{N, C\}$ with asset holding a satisfies the following Hamilton-Jacobi-Bellman (HJB) equation:

$$rV_i^s(a) = z^s\epsilon_i a + \lambda^s(V_i^{s'}(a) - V_i^s(a)) + \delta\pi_j(V_j^s(a) - V_i^s(a)) + \alpha(V_i^s(a_i) - V_i^s(a) - p(a_i - a) - \phi_i(a)) \quad (1)$$

This equation is intuitive. At some poisson rate λ^s, customers in the aggregate state s switch to the other aggregate state s'. At the poisson rate δ, customers of type i changes to type j with probability π_j. And finally, customers meet with dealers at the rate of α. Upon contact, customers and dealers will negotiate trade quantities and an intermediation fee ϕ,

I model the impact of regulations through the following two channels in a stylized fashion. First, the speed at which customers meet with dealers, $\alpha(I)$, increases with the level of dealer inventory I, where $I < \bar{I}$ is the total balance sheet capacity. This captures the immediacy dimension of liquidity. In normal times when buy and sell orders are relatively balanced, higher dealer inventory facilitates faster execution and reduces search times for customers. This is a standard feature in search-based models of OTC markets (e.g., Lagos and Rocheteau 2007).[2] Second, the rate at which the market recovers from a crisis state to a normal state, $\lambda^C(\bar{I} - I)$, is an increasing function of the dealers' unused or "spare" balance sheet capacity, $\bar{I} - I$. This captures the resiliency dimension of liquidity. A lower inventory level I in normal times implies a larger buffer $\bar{I} - I$ that can be deployed during a crisis when strong, one-sided selling pressure requires dealers to have ample spare balance sheet capacity to absorb these flows. A dealer with low capacity $I \approx \bar{I}$ may be forced to sell into

[2]The inventory level in this model is closer to the notion of dealer measure in Lagos and Rocheteau (2007) framework.

the crash, further destabilizing the market. By contrast, a well-capitalized dealer with significant spare capacity can lean against the wind, making the market more resilient to aggregate shocks and facilitating a faster recovery.

I provide two complementary microfoundations for this relationship in the appendix. Appendix B.1 formalizes the "leaning against the wind" channel, where dealers with greater spare capacity can more effectively step in to absorb systemic selling pressure, thereby stabilizing prices and accelerating the recovery to the normal state. In Appendix B.2, I show the same outcome arises by imposing a Stressed Value-at-Risk (SVaR) constraint. Such constraints force dealers to hold less inventory in normal times by requiring them to capitalize against a stressed scenario. Consequently, when a real crisis hits and market volatility spikes, these dealers are inherently more stable and less prone to forced deleveraging. Their continued ability to provide liquidity prevents a complete market collapse and facilitates a faster return to normalcy. Both channels formalize the same tradeoff: by reducing I in normal times regulations enhance resiliency by increasing the effective capacity $\bar{I}-I$ during a crisis. More broadly, this spare capacity $\bar{I}-I$ represents the enhanced, state-contingent risk-bearing capacity that dealers accumulate under regulation. To illustrate, consider a simple linear specification of $\alpha(\cdot)$ and $\lambda^C(\cdot)$. A regulation-induced reduction in dealer inventory in normal times from $I = 80\%\bar{I}$ to $I = 20\%\bar{I}$ would cause trading delays in normal times to quadruple. On the other hand, it would also allow the market to recover from the aggregate liquidity shock four times faster.[3]

As is shown in Lagos and Rocheteau (2007), price in the aggregate state s satisfies the following equation:

$$p^s = \frac{\bar{\epsilon}_H^s}{r} - \frac{\kappa\lambda^s}{r(r+\kappa)(r+\lambda^C+\lambda^N)}(\bar{\epsilon}_H^s - \bar{\epsilon}_H^{s'}) \tag{2}$$

where $\bar{\epsilon}_H^s = \frac{(r+\kappa+\lambda^{s'})z^s+\lambda^s z^{s'}}{r+\kappa+\lambda^C+\lambda^N}\bar{\epsilon} + \frac{r+\kappa}{r+\kappa+\delta}\frac{(r+\kappa+\delta+\lambda^{s'})z^s+\lambda^s z^{s'}}{r+\kappa+\delta+\lambda^C+\lambda^N}(\epsilon_H - \bar{\epsilon})$, $\bar{\epsilon} = \pi_H\epsilon_H + \pi_L\epsilon_L$, $\kappa = \alpha(I)(1-\eta)$ and η is the dealer bargaining power. One useful statistic is the price gap, or absolute price crash $p^N - p^C$ between the normal times and crisis times. Proposition 1 shows how $p^N - p^C$ depends on

[3]The baseline model assumes the trading intensity, α, is constant across aggregate states for tractability. In Appendix B.5, I extend the model to allow for state-dependent search intensities with $\alpha^C < \alpha^N$ and show that the magnitude of the price crash, $p^N - p^C$, is increasing in this trading friction gap $\alpha^N - \alpha^C$ (Figure A4). This suggests that one benefit of better-capitalized dealers may be the ability to prevent a complete collapse in trading during a crisis, thus narrowing this gap and providing a form of inherent or "passive" resilience. By assuming a constant trading intensity $\alpha^N = \alpha^C$, I focus solely on the "active" recovery channel ($\lambda^C(\bar{I} - I)$) in the main text and thus likely provide a conservative estimate of the resiliency benefits of post-GFC regulations.

the recovery speed λ^C and trading speed κ. The proof is in Appendix B.3

PROPOSITION 1. *$p^N - p^C$ decreases in the recovery speed λ^C and increases in the trading speed κ.*

In Figure 1 I plot the trading delays $\frac{1}{\alpha(I)}$ in normal times (N), and percentage drop in price $\frac{p^C - p^N}{p^N}$ and recovery in the stressful times (C) when regulations reduces inventory I from $100\%\bar{I}$ to $20\%\bar{I}$. This is broadly on par with the decline in corporate bond primary dealer inventory from 2006 to 2017-2018.[4] The tradeoff is stark. As shown in the left panel, a lower inventory level reduces the immediacy dimension of liquidity, with trading delays rising in normal times from 1 day to 5 days. However, This loss of immediacy also comes with a huge gain in resiliency. The right panel shows that with more capacity $\bar{I} - I$ to deploy in stress times, the price crash is far less severe (-2.5% vs -9%), and the expected recovery time plummets from two years to just six months.

[Figure 1]

The model suggests that the loss of immediacy and longer trading delays in normal times are the necessary costs in order to have better resiliency in terms of a higher balance sheet capacity ($\bar{I} - I$) to accommodate additional selling pressures in times of stress. It suggests that resiliency itself has two dimensions, the magnitude of a price crash $p^C - p^N$, and the speed that prices recover to normalcy λ^C. I now use this model to evaluate several policy recommendations put forward by the regulators.

2.1 Policy Implication: Electronic Trading

A frequently proposed solution to the decline in immediacy is the adoption of electronic trading platforms (IOSCO 2022). Within the model, this can be viewed as an increase in the trading speed, κ. [5] While this correctly improves immediacy, it cannot address the resiliency dimension of liquidity, as the recovery rate λ^C is unaffected. Furthermore, Proposition 1 shows that a higher trading speed exacerbates the price drop, thereby increasing overall price volatility $\frac{\sqrt{\lambda^N \lambda^C}}{\lambda^N + \lambda^C}(p^N - p^C)$. Thus, while

[4] Goldman Sachs estimates that the level of inventory in 2012 is down 40 percent from the 2006 level (Source: `https://www.ft.com/content/93093b17-8922-3f4f-a0fa-12f9607496f5`). According to the New York Federal Reserve, corporate bond inventory level in 2017-2018 further went down by two-thirds from the 2012 level. Therefore, the level of inventory in 2017-2018 is 20 percent of the 2006 level, on a conservative scale.

[5] One could model electronic trading by introducing a separate trading channel β through which the customers can trade with each other. Then the share of electronic trading is $\frac{\beta}{\alpha(I)+\beta}$,

electronic trading may alleviate the costs of regulation, it does not provide the resiliency benefits and may introduce higher volatility, which may be an undesirable outcome for many fixed-income investors.

2.2 Policy Implication: the Draconian Regulators

The policy recommendation from my model is that corporate bond dealers should remain ready to deploy their additional capacity whenever an aggregate liquidity shock hits the market. Doing so requires regulators to be ready to loosen the constraint on the dealers whenever necessary. I next consider a failure of such state-contingency, representing a 'draconian' regulatory environment. In this scenario, regulations force dealers to hold low inventory ($I << \bar{I}$) in normal times, but rules like the Volcker Rule prevent these dealers from deploying their spare capacity ($\bar{I} - I$) during a crisis. This effectively fixes the recovery rate λ^C at a low level, independent of the dealers' capacity. In Figure 2 I plot this scenario where dealer inventory is reduced to 20% $\bar{I}$, and dealers fail to use the additional capacity in times of crisis: $\bar{I} - I = 0$

[Figure 2]

We see that immediacy during normal times is worsened as trading delays increase from 1 day to 5 days, yet the market gains no resiliency benefit because the spare capacity is never deployed. Prices do not recover faster even if dealers now have the additional capacity to do so. Ironically, the market's recovery dynamics are just as slow as the case when dealers use up all their capacity in normal times $I = \bar{I}$, but without the benefits of high immediacy in normal times. This is the worst of both worlds, and it highlights that the benefits of regulation are contingent on allowing dealers the flexibility to use their spare capacity when it is needed most.

Finally, the right panel of Figure 2 suggests that the two dimensions of liquidity have asymmetric effects on price stability. The magnitude of a price crash is substantially more sensitive to the market's resiliency than to its immediacy. The following proposition formalizes this result, showing that the price gap ($p^N - p^C$) is more elastic with respect to the recovery speed λ^C than with respect to the trading speed κ. The proof is in Appendix B.4.

PROPOSITION 2. *Under reasonable parameter values,* $|\frac{\partial \log(p^N - p^C)}{\partial \log \lambda^C}| > |\frac{\partial \log(p^N - p^C)}{\partial \log \kappa}|$.

3 Empirical Corporate Bond Resiliency

3.1 Data

I use several datasets to comprehensively measure corporate bond liquidity resiliency and the behavior of its participants. Aggregate corporate bond yield spreads are measured using the ICE Bank of America Option-Adjusted Spread indices, available from Federal Reserve Economic Data (FRED). For granular, transaction-level analysis, I use the Academic version of the TRACE database. This dataset provides not only uncensored trading volumes but also masked dealer identifiers, which are essential for constructing dealer-specific measures. To identify the roles of different market participants, I use institutional holdings data from eMAXX, which details the bond positions of insurance companies, mutual funds, and pension funds. Finally, I merge these sources with bond characteristics from the Mergent Fixed Income Securities Database (FISD).

3.2 Improved Resiliency

My theoretical model defines resiliency along two dimensions: the magnitude of the price crash and the speed of the subsequent recovery upon a shock. To measure these two features empirically, I estimate the dynamic response of credit spreads to an aggregate liquidity shock using the local projection method of Jordà (2005) on a weekly basis:

$$\textit{Credit-Spread}_{t+h} = \alpha_h + \beta_h \text{LiqShock}_t + \textit{Lagged Credit-Spread \& VIX} + \epsilon_{t+h} \tag{3}$$

for $h = 0, 1, 2, ...$, where LiqShock measures the aggregate liquidity shocks in the corporate bond market. This regression is rooted in the OTC framework following Weill (2007) and Lagos, Rocheteau, and Weill (2011), where prices drop and rebound in response to an aggregate liquidity shock. I measure this aggregate liquidity shock using the weekly percentage changes in the VIX index. This choice is directly motivated by the microfoundation in Appendix B.2, where a spike in volatility triggers the price crash and subsequent recovery dynamics. In addition, the VIX is a well-established proxy for market-wide fear and has been shown to be a strong driver of aggregate corporate bond liquidity and fund flows (Bao, Pan, and Wang 2011, Goldstein, Jiang, and Ng

2017, Feroli et al. 2014).

I am interested in the evolutions of the coefficients β^h, which trace the cumulative impulse response of credit spreads to a VIX shock over increasing horizons h. A resilient market should exhibit a smaller impact (a lower peak β^h) and a faster decay towards 0. Figure 3 plots these responses for the pre- and post-GFC periods using the aggregate credit spread indices.

[Figure 3]

We see that corporate bond resiliency has improved after 2012 compared to the pre-GFC period. During the 2001-2009 period, 1% VIX shock leads to more than 1% increase in credit spreads. The impact is highly persistent and remains statistically different from zero even after 15 weeks. During the 2012-2020 period, on the other hand, the market response is far more muted and transient. A 1% VIX shock only temporarily increases the credit spread by 0.5%, and the effect becomes statistically insignificant much more quickly, with the 95% confidence bands encompassing zero within just a few weeks.[6] Appendix Figure A5 shows the same improved resiliency after GFC when I run the same local projection regression on a panel of bonds.

My preferred method of measuring resiliency is through these impulse responses by looking at how an aggregate liquidity shock such as VIX spikes is absorbed into prices and how fast price will recover after the shock. To ensure this finding is robust, I corroborate this method with two alternative, well-established measures of resiliency. First, I follow the microstructural approach of Bessembinder et al. (2016), who examine resiliency through the persistent impact of trades on price.[7] For a similar exercise, I estimate the persistent price impact of weekly order flows:

$$\textit{Credit-Yield}_{i,t+h-1} - \textit{Credit-Yield}_{i,t-1} = c_i^h + \lambda_h(-\text{OrderFlow}_{i,t}) + \textit{Lagged OrderFlow \& Credit-Yield}_i + \epsilon_{i,t+h}. \tag{4}$$

A more resilient market should exhibit a smaller and more transient price impact from trades. Figure 4 confirms this pattern. The initial impact of order flow on yields is smaller in the post-

[6] In Figure A6, I add contemporaneous changes in CDS to isolate pure liquidity shocks from VIX. In Figure A9, I plot the 5-week total credit spread response β^5 to liquidity shocks on a rolling window basis. In Figure A10 I plot the response of the liquidity component of credit spreads in response to VIX shocks.

[7] This approach can be unified into the previous framework as trade imbalances can be seen as a proxy for demand shocks Li and Lin (2022). In Appendix Figure A8 I show that bond yields absorb such demand shocks more quickly in the post-GFC period

GFC period compared to the pre-GFC period (0.07 vs. 0.13). The effect also decays much faster in the post-GFC period, becoming statistically insignificant after 10 weeks, while order imbalances continue to impact yields significantly after 20 weeks in the pre-GFC period.

[Figure 4]

Second, following Dong, Kempf, and Yadav 2007, I measure resiliency via the speed of mean-reversion in credit spreads:

$$\Delta \textit{Credit-Spread}_{t+1} = c + \alpha(-\textit{Credit-Spread}_t) + \textit{Lagged } \Delta \textit{ Credit-Spread} + \epsilon_t. \tag{5}$$

This method only measures resiliency by how quickly prices adjust to a shock. It does not tell us the impact of the shock. Nonetheless, a large estimate of the mean reversion rate α represents greater resilience. Consistent with our other findings, Appendix Figure A7 shows that the mean-reversion rate is substantially higher in the post-GFC period. To study the improvement in resilience more closely, it may be useful to translate the mean reversion rate α into half-lives. As a comparison, in Table 1 I follow Barnichon and Matthes (2018) and fit the impulse responses from Equation (3) and (4) to some functional approximation to calculate their corresponding half-lives as well as the maximal impact of the liquidity shock on the yields.

[Table 1]

Across all specifications, the results conclusively suggest an improved resilience in the post-GFC period. Using our primary VIX-based measure (Equation 3), the maximum impact of a shock on credit spreads fell by more than 50% from 0.896 to 0.378, and the half-life of the persistence of the VIX shock plummeted from over 21 weeks to just under 7 weeks. The difference in both parameters is highly statistically significant. The price impact of trades (Equation 4) shows a similar improvement in resiliency, with a significant decline in both impact and persistence. The half-life of the credit spreads according to its mean-reversion rate has also shortened to less than 7 weeks. All three measures of resilience suggest that the corporate bond market has become substantially more resilient in the post-GFC period.

For the remainder of the analysis, I proceed with the VIX-based local projection as the primary measure of resiliency for two crucial reasons. First, it empirically captures the two distinct features of resilience defined by the theoretical model: the magnitude of the price drop (maximum impact of a liquidity shock) and the speed of recovery (half-life). Second, it is directly motivated by the theoretical microfoundation, providing a clear economic channel for the observed dynamics. This focus on the time-based dimensions of liquidity is fundamental to our understanding of the OTC search model. My model is built around two key time-related parameters: the trading delay in normal times and the recovery speed in a crisis. My chosen empirical measure provides a direct counterpart to these parameters, which is essential for conducting the welfare analysis in Section 4.

3.3 Regulations, Dealer Balance Sheet Capacity, and Resiliency

The central hypothesis of my model is that post-GFC regulation is the key driver of improved resiliency in stressful times. This comes at the cost in terms of the worsened immediacy in normal times. Given that previous studies show high-yield (HY) bonds suffered the largest decline in immediacy due to these regulations (e.g., Bao, O'Hara, and Zhou 2018, Wu 2020 etc.), the model predicts that this same segment should exhibit the greatest gains in resiliency. To test this, I estimate the following regression both for high quality AA-rated bonds and for high-yield bond indices across different economic and regulatory periods.

$$\textit{Credit-Spread}_{t+h} = \sum_j \left(c_j^h + \beta_j^h \times \Delta \log(VIX_t) + \textit{Lagged Credit-Spread \& VIX} + \epsilon_{j,t+h} \right) \times \mathbb{1}_{t \in j}, \quad (6)$$

where j is either "pre-GFC" (January 2004 - June 2007), "GFC" (2008), "post-GFC" (Jan 2009 - May 2012), "Regulatory" (June 2012 - Dec 2019), or "COVID" (2020) period, following Choi, Huh, and Shin (2024). Table 2 presents the result.

[Table 2]

Table 2 strongly supports this prediction. The improvement in resiliency is concentrated in the high-yield segment. The "Difference Tests" panel shows that for high-yield bonds, the shock

response coefficients (β^h) in the post-GFC "Regulatory" period are significantly lower than in the "Pre-GFC" period across all horizons (e.g., the difference in β^{10} is -1.066 with a t-statistic of -2.17). A similar statistically significant improvement is also observed when comparing the COVID and GFC periods. By contrast, for high quality AA-rated bonds, the differences between these periods are not statistically significant at conventional levels. This cross-sectional result provides the first piece of evidence for the immediacy-resiliency tradeoff in the OTC market.

The mechanism driving this improved resiliency, according to the model, is the enhanced capacity of better capitalized dealers to act as shock absorbers. I provide evidence for this in two steps. First, I document the enhanced stability of the dealer network itself. In the top panel of Figure 5, I track the volume share of the top 15 dealers (ranked by pre-crisis volume) through two crises. During GFC, the top dealers of 2007 lost significant market share by almost 10 percentage points, suggesting a fragility in the dealers and a disruption of established trading relationships when stress hit. By contrast, the top dealers of 2019 maintained their dominant market presence throughout the 2020 COVID crisis, consistently handling over 50% of transaction volume. This stability of the core dealers shows the improved market resilience in the post-GFC period; it ensures that these primary liquidity providers remain engaged with the market, and are ready to intermediate even in times of crisis.

[Figure 5]

This enhanced stability of the dealer network is not merely a passive phenomenon; it enables of a more active, shock-absorbing role for dealers. In the pre-GFC period, dealers faced low capital requirements, leading them to build up large inventories to facilitate trading and compete for market share in a high-immediacy environment (An 2022). After the great financial crisis, regulations imposed more stringent capital requirements, forcing dealers to hold lower inventory levels during normal times. Consequently, dealers entered the recent crisis better capitalized. This newfound spare capacity meant they were no longer forced to deleverage into a falling market and propagate the systematic shock; instead, they were able to actively provide liquidity and accommodate strong selling pressures when it was needed most. To see how dealers actively managed their inventory in

response to an aggregate liquidity shock, I run the following regression:

$$\log(Inventory_{t+h}) = c^h + \beta^h \times \Delta \log(VIX_t) + Lagged\ log\ Inventory + \epsilon_{t+h} \tag{7}$$

where I use the aggregate corporate bond primary dealer inventory statistics from the New York Federal Reserve. The bottom Panel of Figure 5 plots the impulse response β^h of different horizons.

We see striking evidence of a behavioral shift by dealers in response to VIX shocks. During the GFC, the responses β^h are persistently negative. Corporate bond primary dealers were not able to lean against the wind. In fact, they were doing exactly the opposite, offloading corporate bonds in response to the aggregate liquidity shock, contributing to greater instability in the financial market. This is not the case during the recent COVID pandemic. We see that these primary dealers were able to expand their inventory and increase their corporate bond holdings in response to the same 1% VIX shock. This piece of evidence is consistent with Kargar et al. (2021) who find that dealers were accumulating inventory during COVID. It is also consistent with my model. Before the great financial crisis, dealers hold large amount of inventory, and so they cannot expand their balance sheets further ($I = \bar{I}$). They have to offload some bonds first in order to expand their capacity again (Choi, Shachar, and Shin 2019, Randall 2015). After the great financial crisis, regulations impose a lower inventory level in normal times, which means that dealers now have more balance sheet capacity $\bar{I} - I$ to lean against the wind, precisely when liquidity is needed the most in times of crisis. Furthermore, the market's ability to digest the shock has improved. The impact of 1% VIX shock on dealer inventory during the GFC took over 30 weeks to dissipate, whereas it vanished in half that time during the COVID crisis.

If high yield bonds show greater liquidity resiliency after great financial crisis, it must mean that the dealers now have greater flexibility to expand their balance sheets for the high yield bonds in times of crisis. For this purpose, I look at the corporate bond dealer trade imbalance in a similar spirit to Duffie et al. (2023). We expect to see that for the high yield bonds, corporate bond dealers were able to expand their balance sheet capacity to lean against the wind during COVID, absorbing the selling pressures. To measure the dealer trade imbalance, I use the Academic version of TRACE that includes the masked dealer identities. For each dealer (d) and each bond (i), I first compute

its trade imbalance using dealer-customer trades at the weekly frequency. I then take the average across different dealers of the same bond to get the trade imbalance at the bond level:

$$Imbalance_{i,t} = \frac{1}{D} \sum_{d \in D} \frac{BuyVol_{d,i,t} - SellVol_{d,i,t}}{BuyVol_{d,i,t} + SellVol_{d,i,t}} \tag{8}$$

In figure 6, I plot the time series of the median trade imbalances for investment grade (IG) and high-yield (HY) bonds. We see that in normal times, corporate bond dealers maintain a net zero imbalance, reflecting the relative equal buy or sell requests from the customers in normal times. During the GFC, corporate bond dealers were net sellers of both investment grade and high-yield bonds, resulting in a negative 30% imbalance for both bonds. However, such trends have been reversed during COVID. For high yield bonds, dealers become net buyers and are able to maintain a positive 30% imbalance to absorb the selling pressures during the COVID period.

[Figure 6]

Table 3 confirms this finding statistically. We see that the differences in trade imbalances between investment grade and high yield bonds only become significant after the "Regulatory" period. The net trade imbalance is -4 to -6% on average during the great financial crisis for both investment grade and high yield bonds. Since the COVID pandemic on the other hand, dealers were able to maintain on average a 25% trade imbalance for high-yield bonds, which is more than 20 percentage points increase compared to the pre-GFC period, while such difference is not statistically significant for investment grade bonds. The results suggest that dealers' newfound capability to "lean against the wind" is deployed primarily in the high-yield bond segment.

[Table 3]

Further evidence connecting this behavior to regulation comes from median trade sizes, plotted in Panel B of Figure 6. Following the GFC, average trade sizes declined for both classes of bonds, but the reduction is visibly more pronounced for high yield bonds. This decline in trade size serves as a direct proxy for the reduction in dealer inventory commitment (I) under the new regulatory regime. As outlined in Appendix B.2, regulations like the SVaR constraint impose higher capital

charges on riskier assets, compelling dealers to significantly reduce their normal-time inventory holding and trade size of high yield bonds. Such regulation has two consequences on high yield bond liquidity. On the one hand, lower inventory holding in normal times worsen the immediacy dimension of high yield bonds more than investment grade bonds (Bao, O'Hara, and Zhou 2018, Wu 2020), resulting in longer trading delays and liquidity premium in normal times. On the other hand, it is precisely this larger, regulation-induced reduction in committed capital for high-yield bonds that creates the greater spare capacity ($\bar{I} - I$) needed to enhance their resiliency in times of crisis.

To provide more direct evidence linking regulations to resiliency, I exploit the fact that post-GFC capital rules disproportionately affected the largest dealer banks. I test whether bonds intermediated by these "regulated dealers" saw a greater improvement in their liquidity resiliency compared to bonds traded by smaller dealers. Formally, I test the following:

$$\Delta \textit{Credit-Yield}_{i,t+5} = c_i + \beta \times \log(VIX_t) + \eta \times \log(VIX)_t \times \mathbb{1}_{i,t \in \text{Regulated Dealer}} + \epsilon_{i,t+5}, \qquad (9)$$

where $\mathbb{1}_{i,t \in \text{Regulated Dealers}} = 1$ if over 90% of bond i's trades in week t are done by the top 15 dealers (ranked by the total trading volume in the sample), and $\mathbb{1}_{i,t \in \text{Regulated Dealers}} = 0$ if less than 10% of bond i's trades in week t are done by the top 50 dealers.[8] Table 4 shows that results of this difference-in-differences test.

[Table 4]

We see that the improved liquidity resilience comes from bonds with a majority of trades done by the top 15 dealers.During the 2008 GFC, both groups of bonds were equally fragile, with large and statistically significant 5-week yield responses to a 1% VIX shock. In 2020 on the other hand, while bonds traded by non-regulated dealers remained fragile, the response for bonds traded by regulated dealers became statistically indistinguishable from zero. The formal "COVID - GFC" test statistic for regulated dealers is -3.545 and statistically significant. These results confirm that the improvement in resiliency is likely attributable to the dealers most affected by regulation.

[8] I focus on the top 50 dealers here to create roughly equal number of observations in the regulated dealer sample and the non-regulated dealer sample. Results are robust if I use the top 10 dealers for the non-regulated dealer sample

Figure 7 provides direct evidence for our regulation-driven hypothesis by plotting the accumulated inventory of the Top 15 dealers, our proxy for the most regulated institutions, against the rest of the market. The contrast between the two crises is stark. During the GFC, these top dealers acted pro-cyclically, as their inventories contracted more sharply than those of their smaller counterparts. This pattern reversed entirely during the COVID-19 crisis. While smaller dealers again shed assets, the Top 15 dealers' inventories experienced a far milder initial dip before they decisively increased their holdings, absorbing market-wide selling pressure. This behavioral shift to counter-cyclical intermediation is unique to the highly regulated dealer segment and strongly supports the view that enhanced capitalization was the primary driver of improved market resiliency.

[Figure 7]

Figure 7 provides more visualized evidence for this regulation-driven mechanism. I plot the accumulated inventory for the top 15 dealers—our proxy for the most regulated institutions—against the rest of the dealer community during both crises. The behavioral shift is striking. During the GFC, the inventories of the top 15 dealers contracted more sharply than those of their smaller counterparts, indicating that the primary intermediaries were shedding assets more heavily. This pattern reversed entirely during the COVID-19 crisis. The same top 15 dealers experienced a far milder initial dip in their inventory compared to smaller dealers before they decisively increased their holdings, absorbing market-wide selling pressure. This behavioral shift to counter-cyclical intermediation is unique to the highly regulated dealers and strongly supports the view that enhanced capitalization was the primary driver of improved market resiliency.

3.4 Alternative Explanation

A plausible alternative explanation for the improved resiliency is the changing composition of market participants, with non-dealer institutions such as mutual funds or insurance companies stepping in to provide liquidity. O'Hara, Rapp, and Zhou (2021) show that insurance companies helped support the investment grade bond resiliency during COVID. However, insurance companies

do not trade or hold many high yield bonds due to their regulatory mandates. This makes them an unlikely source for the improved resiliency in the high-yield segment, which is the focus of my findings.

This leaves mutual funds as the other major non-dealer participant. To formally test whether mutual funds contribute to the improved resiliency in the corporate bond market, I utilize the institutional investor holdings data from eMAXX and examine how mutual funds and dealers trade in response to bond rating downgrades or "fallen angel" events (when a bond is downgraded from investment grade to high-yield grade). Such events can be seen as another proxy for liquidity shocks as they often trigger forced selling by mandate-driven investors like insurance companies (Dick-Nielsen and Rossi, 2018). Formally, I follow He, Khorrami, and Song (2022) and estimate the following regression:

$$\Delta(Position)_{i,t} = c + \beta \times Downgrades/Fallen\ Angel_{i,t} + \gamma Controls_{i,t} + Fixed\ Effect_t + \epsilon_{i,t}, \quad (10)$$

where the dependent variable $\Delta(Position)_{i,t}$ is the change in holdings of bond i for mutual funds (from eMAXX) or the order imbalance for dealers (from TRACE), which proxies for the change in their inventory.

[Table 5]

Table 5 presents the results, which rule out mutual funds as a source of improved resiliency and instead reinforce the central role of dealers. We see that when a bond is downgraded or becomes a fallen angel, mutual funds are actually net sellers, reducing their holdings of these downgraded bonds. They act as pro-cyclical traders, adding to the selling pressure rather than absorbing it. Dealer behavior on the other hand, shows a reversal across different regulatory regimes. They remained passive and did not adjust their holdings of the downgraded bonds before 2008, with no significant change in their imbalances. After 2012 when dealer capacity became high, dealers have become net buyers of the downgraded bonds, with their trade imbalance increasing significantly. The evidence suggests that it is the better-capitalized dealers of the post-GFC era, not other institutions, who can actively "lean against the wind" and provide the crucial shock-absorbing capacity that enhances liquidity resiliency in corporate bond market.

4 Welfare Implication

Having established that corporate bond market liquidity now exhibits stronger resiliency and that post-GFC regulations are a potential cause, I now use my model to evaluate the welfare implications of regulations on the OTC market liquidity. Such an analysis is not possible in standard OTC models with a single aggregate state because these models can only feature the costs of regulation (i.e., deteriorating immediacy in normal times) without accounting for the resiliency benefits. To be more specific, the welfare criterion is the average utility of customers across both normal and crisis times:

$$U = \frac{\lambda^C}{\lambda^C + \lambda^N} V^N + \frac{\lambda^N}{\lambda^C + \lambda^N} V^C. \tag{11}$$

where

$$V^N = \mathbb{E}\Big\{ \int_0^{T^N} \big(n_{HH} z^N \epsilon_H a_H^N + n_{HL} z^N \epsilon_L a_H^N\big) e^{-rt} dt + e^{-rT^N} V^C \Big\}$$

and

$$V^C = \mathbb{E}\Big\{ \int_0^{T^C} \big(n_{HH} z^C \epsilon_H a_H^C + n_{HL} z^C \epsilon_L a_H^C\big) e^{-rt} dt + e^{-rT^C} V^N \Big\}.$$

n_{ij} is the distribution of agents with preference type j and asset holding a_i^s. Here the expectation $\mathbb{E}$ is with respect to T^C and T^N, which are exponentially distribution with λ^C and λ^N. Some calculations yield the following analytical formula for customer welfare (per unit of bond supply A):

$$\begin{aligned} \frac{U}{A} &= \frac{\lambda^C(\bar{I} - I) z^N + \lambda^N z^C}{\lambda^C(\bar{I} - I) + \lambda^N} \frac{1}{r} \Big\{ \frac{\delta \pi_H + \alpha(I)}{\alpha(I) + \delta} \epsilon_H + \frac{\delta \pi_L}{\alpha(I) + \delta} \epsilon_L \Big\} \\ &= \frac{1}{r} \mathbb{E}_s[z^s] \mathbb{E}_i[\epsilon_i]. \end{aligned} \tag{12}$$

This welfare function captures the immediacy-resiliency tradeoff. The first component, $\mathbb{E}_s[z^s]$, represents the expected aggregate valuation of the economy. It is increasing in the recovery speed λ^C, which is a function of dealers' capacity $\bar{I} - I$. A lower inventory in normal times increases capacity, raises the recovery speed, and thus increases average welfare by increasing the long-run

share of time the economy stays in the normal state. This term represents the welfare gain from resiliency. The second component, $\mathbb{E}_i[\epsilon_i]$, captures the average utility from holding the bond, which is increasing in the trading speed α. A lower inventory in normal time reduces the trading speed, making it harder for high-valuation investors to acquire bonds and thus lowering the average utility from holdings. This term represents the welfare cost of lost immediacy. The optimal inventory level, therefore, is determined by balancing the marginal benefit of increased resiliency and the marginal cost of reduced immediacy.

I calibrate the model's parameters to quantitatively assess this tradeoff, with the full details summarized in the top panel of Table 6. The calibration strategy is grounded in the empirical evidence presented earlier in the paper and in the corporate bond liquidity literature. Specifically, I set the recovery parameter $\lambda^C(\bar{I} - I)$ to directly match the shock half-lives for the pre-GFC and post-GFC periods estimated in Table 1, assuming the pre-GFC inventory level is at the maximal $I = \bar{I}$, and the post-GFC inventory is $20\%\bar{I}$. Other parameters governing trading friction are chosen to align with empirical moments (e.g., trading delays and average turnover) from Wu (2020) and Feldhütter (2012). Panel B of Table 6 confirms that the model successfully reproduces the liquidity premium in normal times and the price crash in crisis, two key untargeted moments across both the pre- and post-GFC regimes, thereby validating its core mechanism and providing a credible foundation for the welfare analysis.

[Table 6]

In Figure 8 I plots the several outcomes of the calibrated model as a function of dealers' spare balance sheet capacity ($\bar{I} - I$). The figure clearly illustrates the two opposing effects of post-GFC regulation. As spare capacity increases from 0 to 80% (i.e., dealer inventory I falls to 20%), the costs of regulation manifest as longer trading delays from 1 day to 5 days and a higher normal-time liquidity premium, which rises from 6 to 24 basis points. Both are consistent with their empirical counterparts reported in Wu (2020). Simultaneously, the market gains resiliency, evidenced by a significant reduction in the crisis-time price crash from 5.6% to 1.9%. The welfare function in the bottom panel balances these costs and benefits. Interestingly, the welfare gains from enhanced resiliency initially dominate the costs from lost immediacy. The analysis reveals that investor

welfare is maximized when spare balance sheet capacity is around 80% of the total, which implies an optimal dealer inventory level of 20%. This model-driven result is strikingly consistent with the actual dealer inventory level reduction observed in the post-GFC era.

[Figure8]

While the model is stylized, its implications should be interpreted broadly. The concept of an optimal dealer capacity $(\bar{I} - I)$ maps directly to other quantifiable regulatory levers. For instance, it can inform the optimal reduction in permissible trade sizes or the degree to which dealers must capitalize against a GFC-like stress scenario, as formalized in the SVaR microfoundation in Appendix B.2. Regulators can therefore look to these more direct observables to guide the design of policy. This analysis also underscores the peril of improperly designed rules. In a "draconian" Volcker-like regime where capital requirements are tight in normal times but are not relaxed during a crisis (effectively fixing λ^C at a low level), reducing dealer inventory I would be unambiguously welfare-reducing (Figure A11). Investors would suffer the costs of lower immediacy without reaping any resiliency benefits. This highlights the critical importance of state-contingency: the balance sheet capacity stored during normal times must be deployed when it is most needed, making a flexible regulatory framework essential for overall market welfare.

4.1 Counterfactual: The Role of Regulation in the Fed's COVID-19 Intervention

The model's ability to distinguish between the market's intrinsic resiliency and external government interventions allows me to conduct an interesting and crucial counterfactual exercise: how effective would the Federal Reserve's unprecedented 2020 corporate credit facilities have been in a less resilient, pre-GFC regulatory environment? To formally separate these effects, I model the total recovery speed from a crisis, λ^C, as the sum of the market's intrinsic capacity and an external policy boost:

$$\lambda^C = \lambda_0 + \lambda_1(\bar{I} - I) + \lambda_{Fed}. \tag{13}$$

In this framework, $\lambda_0 + \lambda_1(\bar{I} - I)$ represents the market's internal recovery capacity, which is a direct function of the regulatory regime through its effect on dealers' spare capacity $(\bar{I} - I)$. The

additional λ_{Fed} captures the exogenous impact of the central bank's intervention. This structure allows me to isolate the contribution of the underlying market structure by applying the same policy shock (λ_{Fed}) to different regulatory environments, thereby quantifying the complementarity between regulation and central bank action.

To estimate the marginal impact of the Fed's intervention, λ_{Fed}, I run the local projection (3) on two nested sub-periods: the period just before the Fed's major announcements (January 2019 - March 20th, 2020) and the period after (March 20th, 2020 - June 2021). Panel A of Table 7 shows the Fed's intervention significantly increases in the annualized recovery speed from 5.39 to 7.50. The difference implies an additional $\lambda_{Fed} = 2.11$, which serves as our measure of the Fed's direct intervention effect. We then apply this measure of the Fed's intervention effect to different regulatory regimes in Panel B of Table 7. In Scenario 1 (Actual), the Fed's intervention is applied to the resilient, post-GFC market structure with $\lambda_0 + \lambda_1(\bar{I} - I) = 5.25$ and $I = 0.8\bar{I}$. The total recovery speed rises to 7.36 (i.e., 5.25 + 2.11), corresponding to a shock half-life of just 4.90 weeks and a modest price crash of -1.35%. In Scenario 2 (Counterfactual), the same Fed intervention ($\lambda_{Fed} = 2.11$) is applied to the fragile, pre-GFC market structure with no spare dealer capacity ($\lambda_0 = 1.70$ and $I = \bar{I}$). The total recovery speed can only reach 3.81 (i.e., 1.70 + 2.11), resulting in a shock half-life of 9.46 weeks—nearly double that of the actual scenario. More dramatically, the price crash deepens to -2.56%, an impact almost twice as severe.

[Table 7]

This analysis demonstrates that the post-GFC regulatory framework did more than just enhance baseline resiliency; it effectively multiplied the power of the Federal Reserve's crisis-fighting tools. The very same intervention was twice as effective at stabilizing prices and halved the market's recovery time simply because it was acting on a foundation of better-capitalized intermediaries. This suggests that the welfare benefits of regulation, as outlined in this paper, extend beyond intrinsic market stability to include the enhanced efficacy of public-sector backstops.

5 Conclusion

Post-GFC regulations on corporate bond dealers create a tradeoff between immediacy in normal times and resiliency in times of crisis. Reduced immediacy and dealer inventory in normal times are the necessary costs of the enhanced market resiliency in times of stress. In this paper, I show that better-capitalized dealers are able to "lean against the wind", absorbing systemic liquidity shocks and stabilizing prices, which lead to a faster recovery. This effect is particularly pronounced for high-yield bonds, which have experienced the largest declines in immediacy but also the greatest improvements in resiliency, driven by dealers' increased balance sheet capacity. These findings challenge the prevailing narrative that post-GFC regulations have unambiguously harmed market liquidity. Rather, these regulations have created a necessary balance, trading off some immediacy in normal times for greater resiliency during crises.

I developed a stylized OTC model that links lower dealer inventories in normal times to greater balance sheet capacity during crises. This framework allows one to conduct a comprehensive welfare analysis to evaluate the impact of post-GFC regulations on market liquidity. Overall, my findings underscore the importance of maintaining flexibility in regulatory frameworks, allowing dealers to utilize their balance sheet capacity effectively when liquidity is needed the most. These insights are particularly relevant for policymakers aiming to enhance market stability and investor welfare. Future studies could further explore the dynamic interactions between regulatory constraints, dealer behavior, and market outcomes, providing additional guidance for designing resilient financial systems.

References

Adrian, Tobias, Michael Fleming, Or Shachar, and Erik Vogt. 2017. "Market Liquidity After the Financial Crisis." *Annual Review of Financial Economics* 9 (1):43–83.

Afonso, Gara. 2011. "Liquidity and congestion." *Journal of Financial Intermediation* 20 (3):324–360.

An, Yu. 2022. "Competing with Inventory in Dealership Markets." Working Paper No. 3284836. SSRN.

Bao, Jack, Maureen O'Hara, and Xing (Alex) Zhou. 2018. "The Volcker Rule and corporate bond market making in times of stress." *Journal of Financial Economics* 130 (1):95–113.

Bao, Jack, Jun Pan, and Jiang Wang. 2011. "The Illiquidity of Corporate Bonds." *The Journal of Finance* 66 (3):911–946.

Barnichon, Regis, and Christian Matthes. 2018. "Functional Approximation of Impulse Responses." *Journal of Monetary Economics* 99:41–55.

Becker, Bo, and Efraim Benmelech. 2021. "The REsilience of the U.S. Corporate Bond Market During Financial Crisis." Working Paper No. 28868. National Bureau of Economic Research.

Bessembinder, Hendrik, Allen Carrion, Laura Tuttle, and Kumar Venkataraman. 2016. "Liquidity, resiliency and market quality around predictable trades: Theory and evidence." *Journal of Financial Economics* 121 (1):142–166.

Bessembinder, Hendrik, Stacey Jacobsen, William Maxwell, and Kumar Venkataraman. 2018. "Capital Commitment and Illiquidity in Corporate Bonds." *The Journal of Finance* 73 (4):1615–1661.

Boyarchenko, Nina, Anna Kovner, and Or Shachar. 2022. "It's what you say and what you buy: A holistic evaluation of the corporate credit facilities." *Journal of Financial Economics* 144 (3):695–731.

Chaudhary, Manav, Zhiyu Fu, and Jian Li. 2022. "Corporate Bond Multipliers: Substitutes Matter." Working Paper No. 4292266. SSRN.

Choi, Jaewon, Yesol Huh, and Seunghun Shin. 2024. "Customer Liquidity Provision: Implications for Corporate Bond Transaction Costs." *Management Science* 70 (1):187–206.

Choi, Jaewon, Or Shachar, and Seunghun Shin. 2019. "Dealer Liquidity Provision and the Breakdown of the Law of One Price: Evidence from the CDS–Bond Basis." *Management Science* 65 (9):4100–4122.

Cohen, Assa, Mahyar Kargar, Benjamin Lester, and Pierre-Olivier Weill. 2024. "Inventory, market making, and liquidity in OTC markets." *Journal of Economic Theory* 222:105917.

Dick-Nielsen, Jens, and Marco Rossi. 2018. "The Cost of Immediacy for Corporate Bonds." *The Review of Financial Studies* 32 (1):1–41.

Dong, Jiwei, Alexander Kempf, and Pradeep K. Yadav. 2007. "Resiliency, the Neglected Dimension of Market Liquidity: Empirical Evidence from the New York Stock Exchange." Working Paper No. 967262. SSRN.

Driscoll, John, and Aart Kraay. 1998. "Consistent Covariance Matrix Estimation With Spatially Dependent Panel Data." *The Review of Economics and Statistics* 80 (4):549–560.

Du, Wenxin, Benjamin Hébert, and Wenhao Li. 2023. "Intermediary balance sheets and the treasury yield curve." *Journal of Financial Economics* 150 (3):103722.

Duffie, Darrell, Michael Fleming, Frank Keane, Claire Nelson, Or Shachar, and Peter Van Tassel. 2023. "Dealer Capacity and U.S. Treasury Market Functionality." Staff Report No. 1070. Federal Reserve Bank of New York.

Duffie, Darrell, Nicolae Gârleanu, and Lasse Heje Pedersen. 2005. "Over-the-Counter Markets." *Econometrica* 73 (6):1815–1847.

Duffie, Darrell, Nicolae Gârleanu, and Lasse Heje Pedersen. 2007. "Valuation in Over-the-Counter Markets." *The Review of Financial Studies* 20 (6):1865–1900.

Feldhütter, Peter. 2012. "The Same Bond at Different Prices: Identifying Search Frictions and Selling Pressures." *The Review of Financial Studies* 25 (4):1155–1206.

Feroli, Michael, Anil Kashyap, Kermit Schoenboltz, and Hyun Song Shin. 2014. "Market Tantrums and Monetary Policy ." Forum report no. Proceedings of the U.S. Monetary Policy Forum.

Gilchrist, Simon, Bin Wei, Vivian Z. Yue, and Egon Zakrajšek. 2024. "The Fed takes on corporate credit risk: An analysis of the efficacy of the SMCCF." *Journal of Monetary Economics* 146:103573.

Goldstein, Itay, Hao Jiang, and David T. Ng. 2017. "Investor flows and fragility in corporate bond funds." *Journal of Financial Economics* 126 (3):592–613.

Gârleanu, Nicolae, and Lasse Heje Pedersen. 2007. "Liquidity and Risk Management." *American Economic Review* 97 (2):193–197.

He, Zhiguo, Paymon Khorrami, and Zhaogang Song. 2022. "Commonality in Credit Spread Changes: Dealer Inventory and Intermediary Distress." *The Review of Financial Studies* 35 (10):4630–4673.

He, Zhiguo, Stefan Nagel, and Zhaogang Song. 2022. "Treasury inconvenience yields during the COVID-19 crisis." *Journal of Financial Economics* 143 (1):57–79.

Hugonnier, Julien, Benjamin Lester, and Pierre-Olivier Weill. 2019. "Frictional Intermediation in Over-the-Counter Markets." *The Review of Economic Studies* 87 (3):1432–1469.

IOSCO. 2022. "Corporate Bond Markets – Drivers of Liquidity During COVID-19 Induced Market Stresses ." Discussion Paper No. OR02. International organization of Securities Commissions.

Jordà, Òscar. 2005. "Estimation and Inference of Impulse Responses by Local Projections." *American Economic Review* 95 (1):161–182.

Kargar, Mahyar, Benjamin Lester, David Lindsay, Shuo Liu, Pierre-Olivier Weill, and Diego Zúñiga. 2021. "Corporate Bond Liquidity during the COVID-19 Crisis." *The Review of Financial Studies* 34 (11):5352–5401.

Kargar, Mahyar, Benjamin Lester, Sèbastien Plante, and Pierre-Olivier Weill. 2024. "Sequential Search for Corporate Bonds." *Journal of Finance Forthcoming.*

Lagos, Ricardo, and Guillaume Rocheteau. 2007. "Search in Asset Markets: Market Structure, Liquidity, and Welfare." *American Economic Review* 97 (2):198–202.

Lagos, Ricardo, and Guillaume Rocheteau. 2009. "Liquidity in Asset Markets With Search Frictions." *Econometrica* 77 (2):403–426.

Lagos, Ricardo, Guillaume Rocheteau, and Pierre-Olivier Weill. 2011. "Crises and liquidity in over-the-counter markets." *Journal of Economic Theory* 146 (6):2169–2205.

Li, Jiacui, and Zihan Lin. 2022. "Price Multipliers are Larger at More Aggregate Levels." Working Paper No. 4038664. SSRN.

Lou, Dong. 2012. "A Flow-Based Explanation for Return Predictability." *The Review of Financial Studies* 25 (12):3457–3489.

Newey, Whitney K., and Kenneth D. West. 1987. "A Simple, Positive Semi-Definite, Heteroskedasticity and Autocorrelation Consistent Covariance Matrix." *Econometrica* 55 (3):703–708.

O'Hara, Maureen, Andreas C. Rapp, and Xing (Alex) Zhou. 2021. "The Value of Value Investors." Working Paper No. 4151934. SSRN.

O'Hara, Maureen, and Xing (Alex) Zhou. 2021. "Anatomy of a liquidity crisis: Corporate bonds in the COVID-19 crisis." *Journal of Financial Economics* 142 (1):46–68.

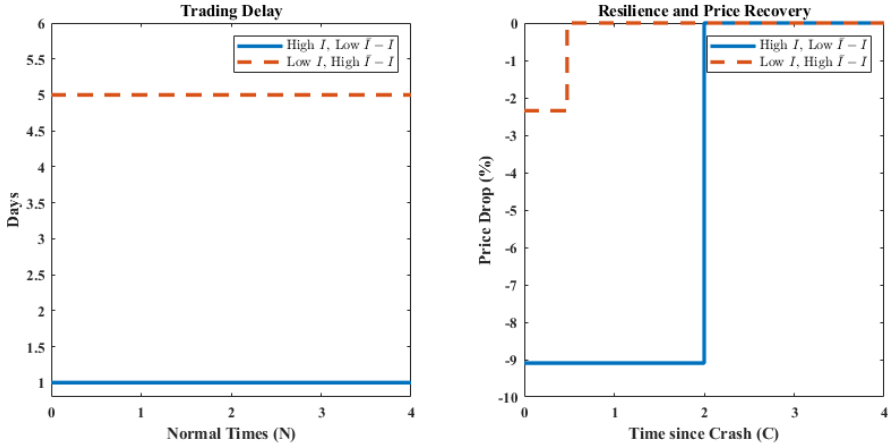
Randall, Oliver. 2015. "How Do Inventory Costs Affect Dealer Behavior in the US Corporate Bond Market?" Working Paper No. 2590331. SSRN.

Weill, Pierre-Olivier. 2007. "Leaning against the Wind." *The Review of Economic Studies* 74 (4):1329–1354.

Wu, Botao. 2020. "Post-Crisis Regulations, Trading Delays, and Increasing Corporate Bond Liqudity Premium." Working Paper No. 3613379. SSRN.

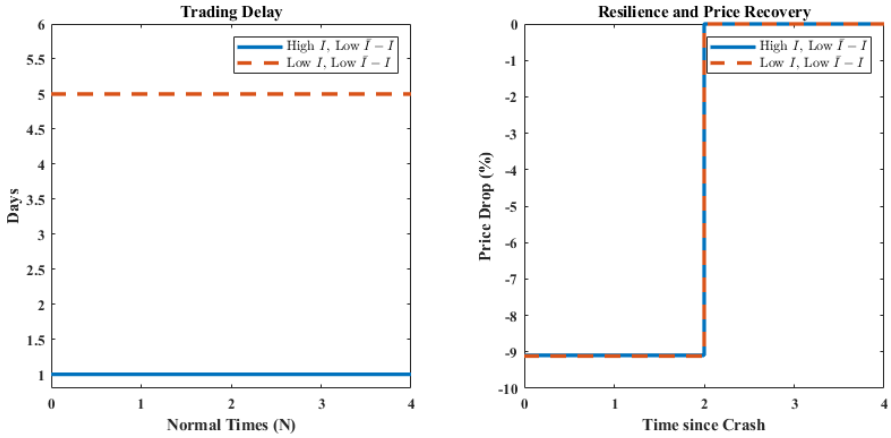
A Figures

Figure 1: Immediacy vs. Resiliency



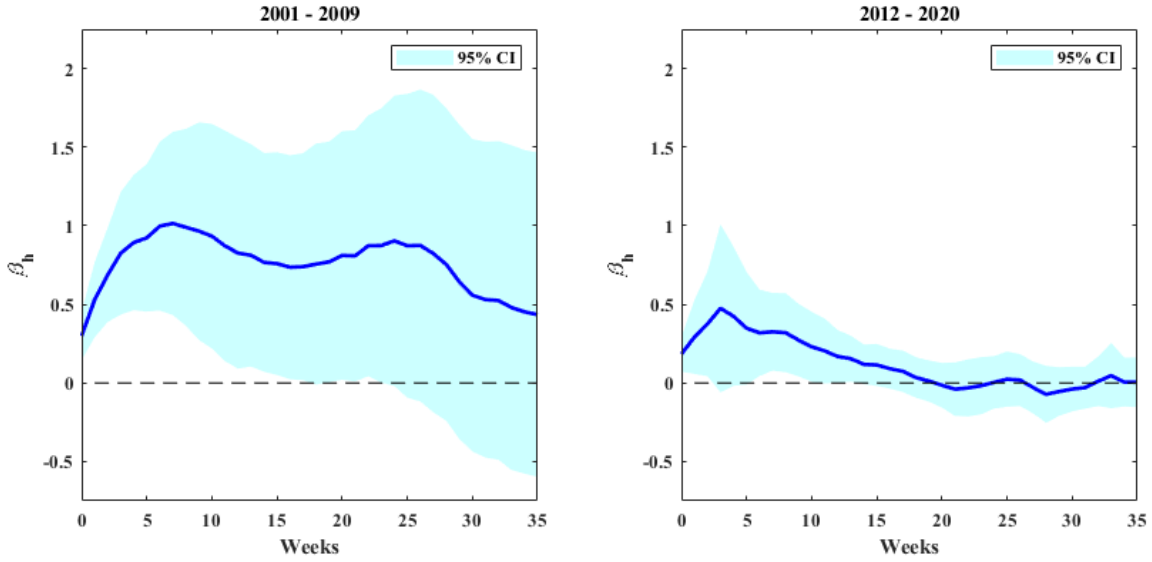
Notes: The left panel shows trading delays in the high inventory $I = \bar{I}$ and low balance sheet capacity $\bar{I} - I = 0$ case (blue solid) vs. low inventory $I = 0.2\bar{I}$ and high balance sheet capacity $\bar{I} - I = 0.8\bar{I}$ case (red dashed). The right panel shows the price recovery in the high inventory and low capacity case (blue solid) vs. low inventory and high balance sheet capacity case (red dashed). Parameters are: $\bar{I} = 1$, $\lambda^N = 0.1$, $\lambda^C = 2 \cdot (\bar{I} - I) + 0.5$, $\epsilon_H = 5$,$\epsilon_L = 0$, $z^N = 1$, $z^C = 0$, $r = 0.05$, $\delta = 3.58$, $\pi_L = 0.33/\delta$, $\eta = 0.9$, $\alpha = 250 \cdot I$.

Figure 2: Immediacy vs. Resiliency when Inventory and Balance Sheet Capacity are Both Low.



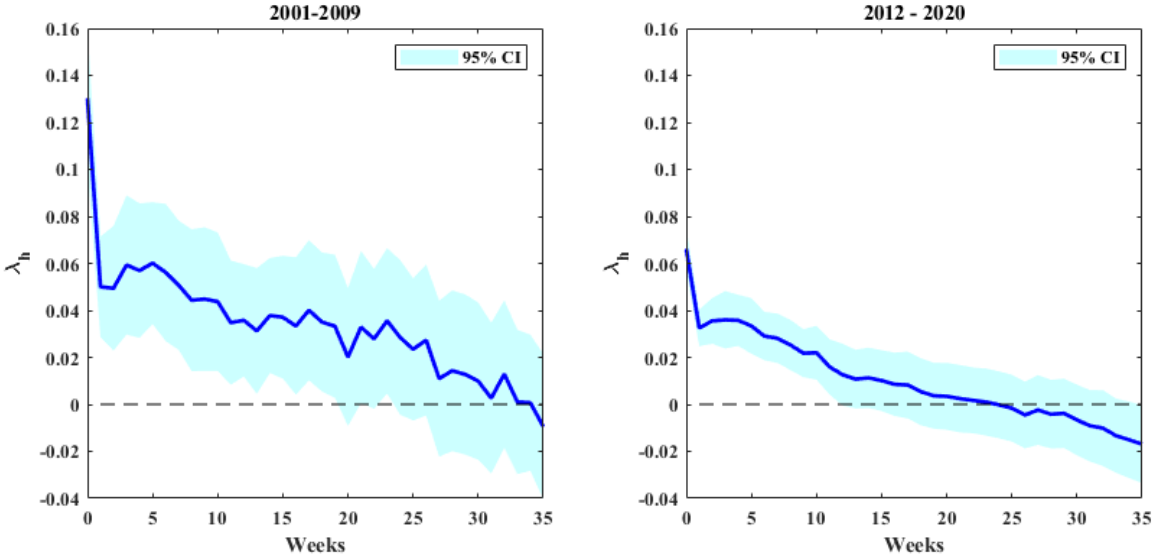
Notes: This figure plots the trading delays and price recovery when both the inventory is low ($I = 0.2\bar{I}$), and dealers fail to use the additional balance sheet capacity in times of stress ($\bar{I} - I = 0$). Parameters are: $\bar{I} = 1$, $\lambda^N = 0.1$, $\lambda^C = 0.5$, $\epsilon_H = 5$, $\epsilon_L = 0$, $z^N = 1$, $z^C = 0$, $r = 0.05$, $\delta = 3.58$, $\pi_L = 0.33/\delta$, $\eta = 0.9$, $\alpha = 250 \cdot I$.

Figure 3: Corporate Bond Resiliency: Aggregate Indices



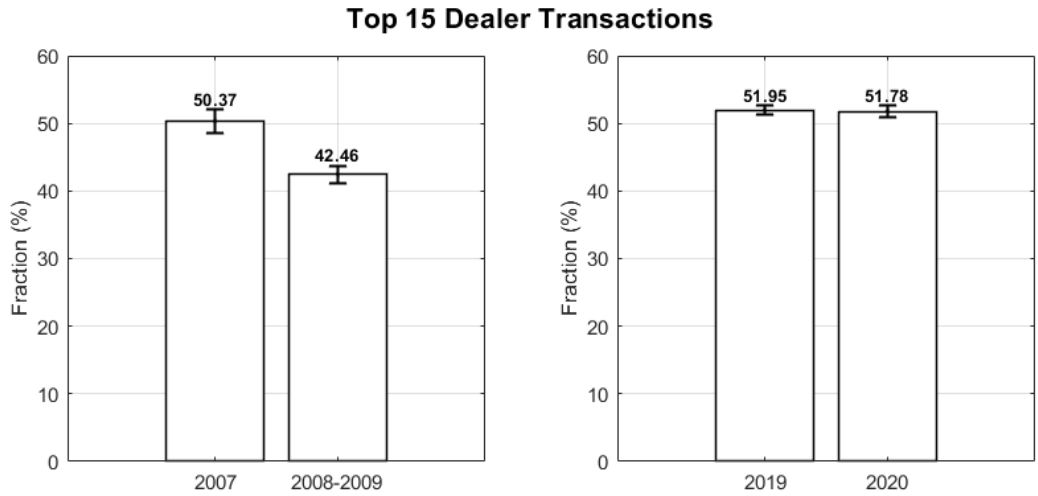
Notes: This figure shows the weekly β^h from Regression 3, as well as the 95% of the confidence intervals using the Newey and West (1987) type of standard errors. The regression is run on the 2001-2009 sample (left), and the 2012-2020 sample (right) respectively.

Figure 4: Corporate Bond Resiliency: Alternative Measure

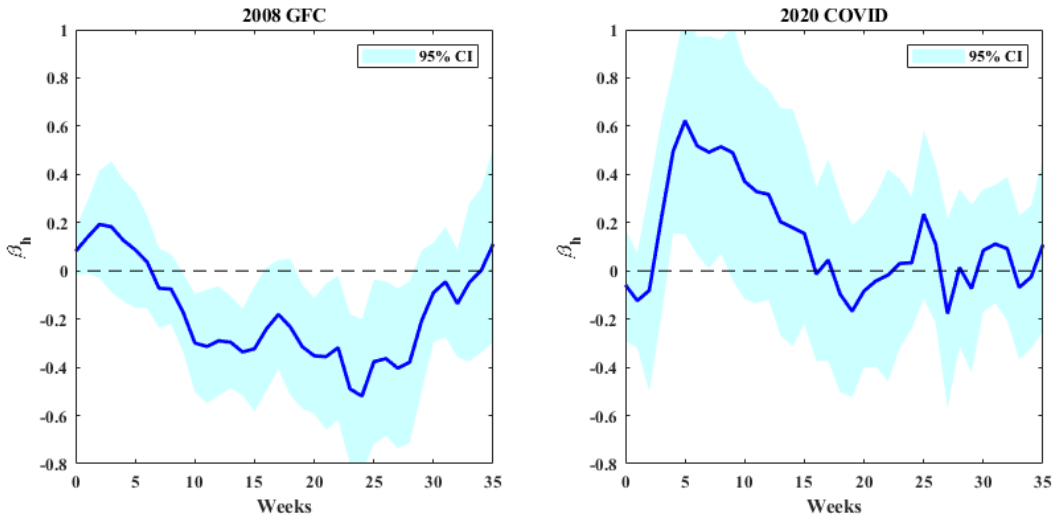


Notes: This figure shows the weekly λ^h from Regression 4, as well as the 95% of the confidence intervals with Driscoll and Kraay (1998) type of standard errors with bond fixed effect. The regression is run on the 2001-2009 sample (left), and the 2012-2020 sample (right) respectively.

Figure 5: Corporate Bond Resiliency: Dealer Stability and Inventory.

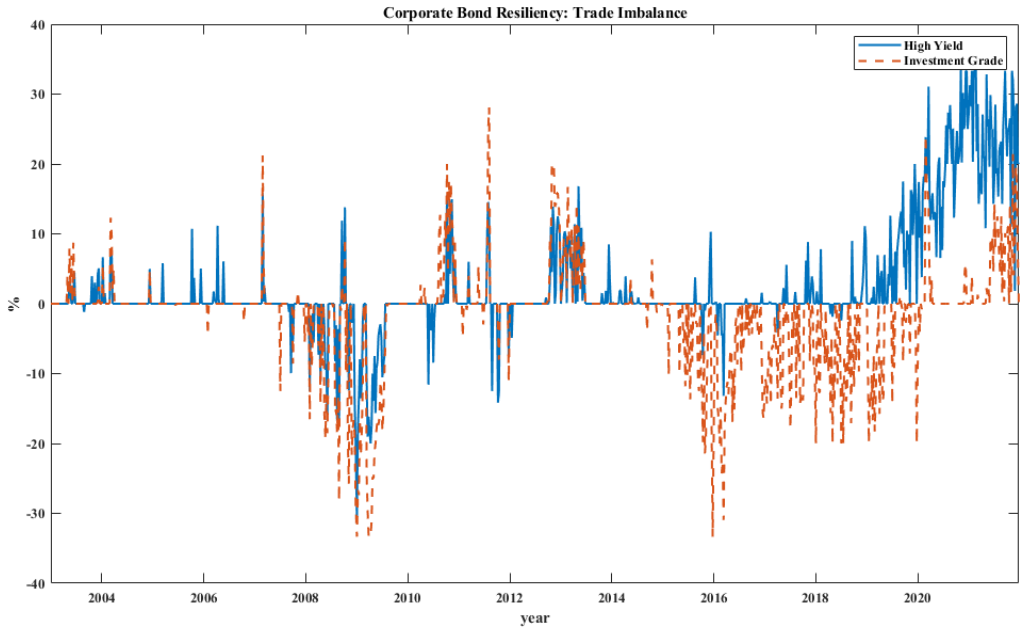


(a) *Notes*: This Figure presents the percentage of trades that are done during crisis by the top 15 dealers ranked by transaction volumes in 2007 (Left) and 2019 (Right).

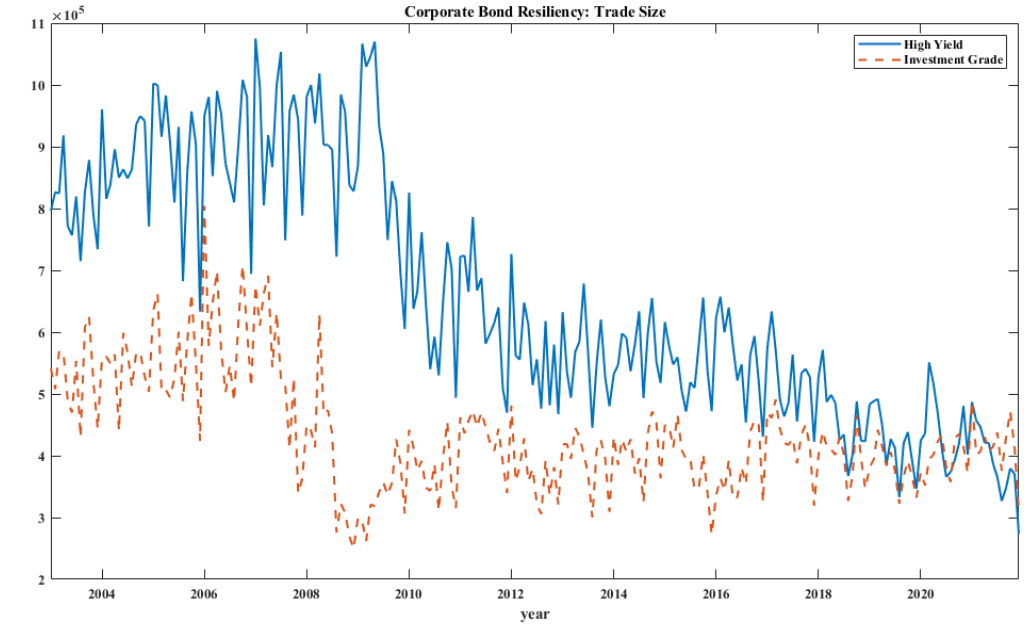


(b) *Notes*: This figure shows the weekly β^h from Regression 7 as well as the 95% confidence interval with Newey and West (1987) types of standard errors. The regression is run on the 2008 sample (left), and the 2020 sample(right) respectively.

Figure 6: Corporate Bond Resiliency: Trade Imbalance and Size.

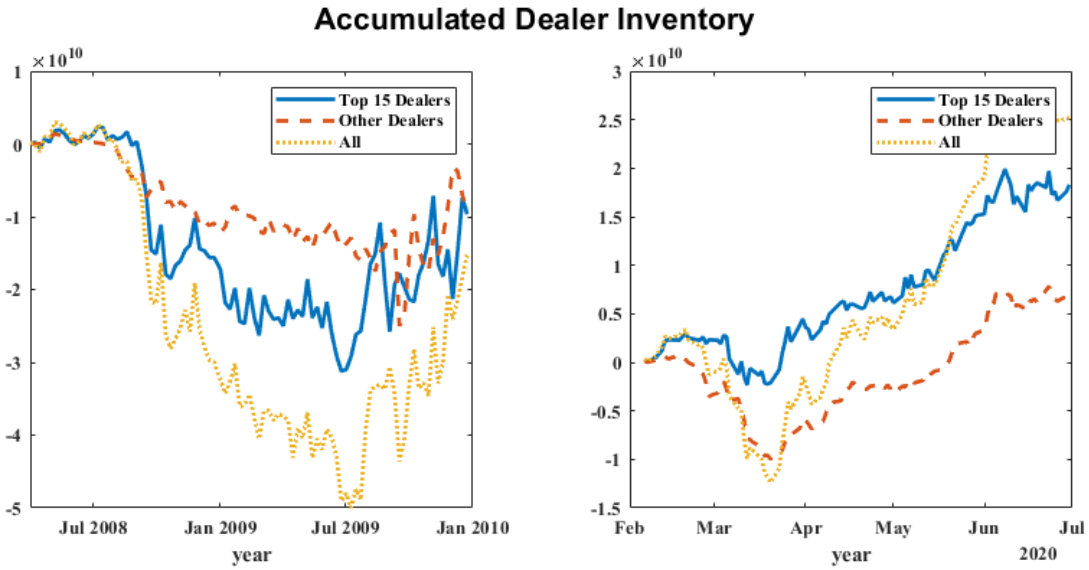


(a) *Notes*: This figure shows the median of the trade imbalances of investment grade and high-yield bonds. Trade imbalance at the dealer-bond-week level is computed from Equation (8). I take average imbalances across different dealers to get the imbalance at the bond-week level, and then plot the cross-sectional median.



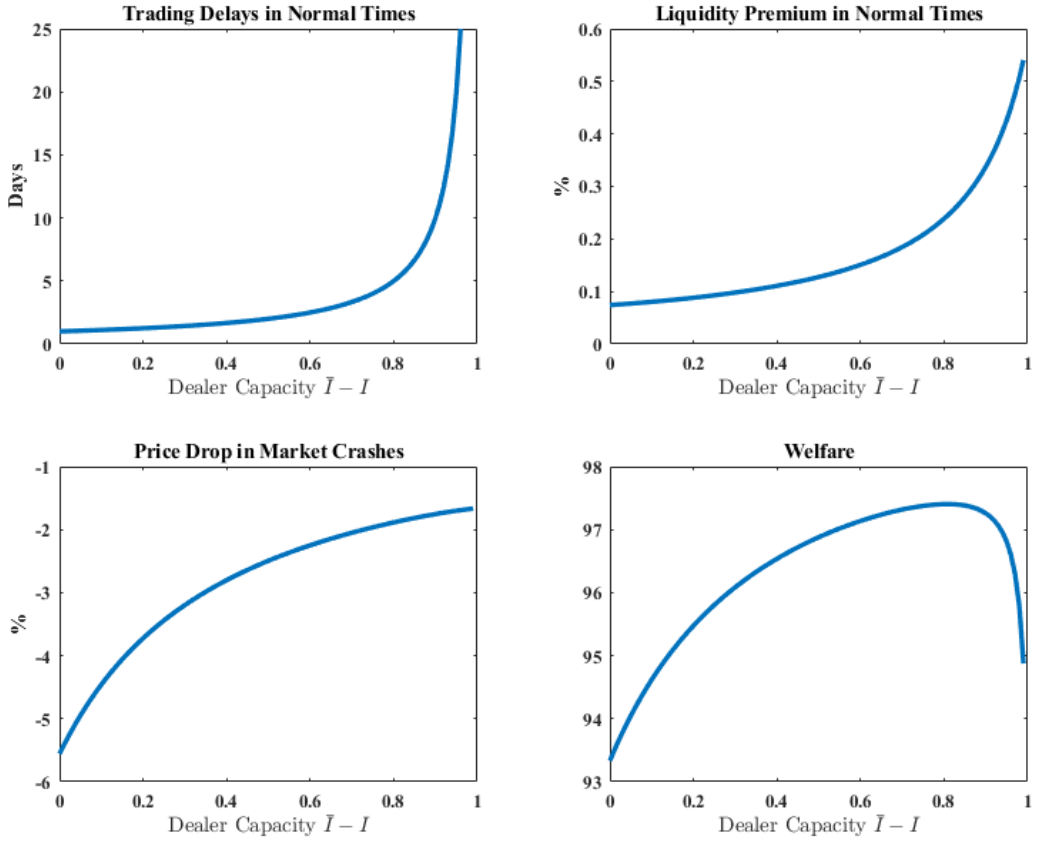
(b) *Notes*: This figure shows the median trade size of investment grade and high yield bonds at the monthly frequency. Trade size is defined as monthly trading volume divided by the number of trades of that month.

Figure 7: Top 15 Corporate Bond Dealer Accumulated Inventory vs. Rest



Notes: This figure shows the accumulated corporate bond dealer inventory for the top 15 dealers (solid blue) and the rest (dashed red) during the Great Financial Crisis (GFC) and COVID. Top 15 dealers are proxies for the dealers subject to the post-GFC regulations.

Figure 8: Welfare



Notes: This figure plots the trading delay in normal times $\frac{1}{\alpha(I)}$, the liquidity premium in normal times $\frac{z^H \epsilon_H}{p^N} - r^N$, price drop in times of crisis $\frac{p^C - p^N}{p^N}$, as well as the welfare in equation (12) as a function of the dealer balance sheet capacity $\bar{I} - I$. Parameters values are from Table 6, and $r = 0.1$ to match the average duration of 10 years, $\epsilon_H = 10$, $\epsilon_L = 4$.

Tables

Table 1: Different Measures of Improved Resiliency

	2001–2009		2012–2020		Difference	
Parameter	Estimate	(t-stat)	Estimate	(t-stat)	Diff.	(t-stat)
Equation (3): $\beta^h = a \exp\left(\frac{-(h-b)^2}{c^2}\right)$						
Maximum Impact	0.896***	(27.19)	0.378***	(23.73)	0.519***	(14.16)
Half-Life (weeks)	21.240***	(9.62)	6.867***	(12.96)	17.264***	(6.33)
Equation (4): $\lambda^h = a \exp(-bh)$						
Maximum Impact	0.080***	(13.05)	0.055***	(12.05)	0.024***	(3.18)
Half-Life (weeks)	11.677***	(8.03)	5.468***	(7.98)	6.210***	(3.86)
Equation (5)						
Maximum Impact (N/A)	—	—	—	—	—	—
Half-Life (weeks)	10^3	(0.04)	6.839**	(2.31)	—	

Notes: This table presents the impulse responses estimated from three different models over two distinct sample periods. "Maximum Impact" refers to the peak of the impulse response function. "Half-Life" measures the number of periods it takes for the impulse response to decay to half of its peak value according to the functional forms. T-statistics are reported in parentheses. For the mean-reversion model, the concept of "maximum impact" from an external shock is not applicable.

Table 2: Comparison of Credit Spread Resiliency Across Ratings

	AA-rated			High Yield		
Period	h=1	h=5	h=10	h=1	h=5	h=10
Pre-GFC (2001.1–2007.12)	0.148***	0.209***	0.113	1.372***	1.878***	1.651***
	(4.35)	(3.34)	(1.37)	(7.23)	(5.24)	(3.75)
GFC (2008.1–2008.12)	1.207***	1.411**	0.731	5.237***	9.748***	11.304**
	(4.36)	(2.49)	(0.87)	(5.10)	(3.81)	(2.47)
Post-GFC (2009.1–2012.5)	0.437***	0.709***	0.533***	1.852***	2.302***	1.914***
	(5.90)	(4.40)	(2.64)	(7.14)	(5.06)	(3.20)
Regulatory (2012.6–2019.12)	0.093***	0.102***	0.072**	0.836***	0.674***	0.585***
	(8.19)	(3.71)	(2.19)	(7.46)	(3.56)	(2.67)
COVID (2020.1–2020.12)	0.686***	0.424	-0.092	2.576***	2.655**	0.760
	(2.63)	(1.20)	(-0.30)	(4.52)	(2.15)	(0.70)
Difference Tests:						
Regulatory vs. Pre-GFC	-0.055	-0.108	-0.041	-0.536**	-1.204***	-1.066**
	(-1.53)	(-1.58)	(-0.46)	(-2.43)	(-2.97)	(-2.17)
COVID vs. GFC	-0.521	-0.987	-0.822	-2.661**	-7.093**	-10.544**
	(-1.37)	(-1.48)	(-0.92)	(-2.27)	(-2.50)	(-2.24)

Notes: This table presents the impulse response coefficients (β_h) from Regression 6 for AA-rated and high-yield bond indices at horizons of 1, 5, and 10 weeks. T-statistics based on Newey and West (1987) type of standard errors, are reported in parentheses. *** (**) [*] denotes statistical significance at 1% (5%) [10%] level.

Table 3: Dealer Trade Imbalance

	Investment Grade (IG)	High Yield (HY)	HY - IG
Period	(1)	(2)	(3)
Pre-GFC: 2003.1 - 2007.12	2.433	2.939	0.507
	(1.01)		(1.01)
GFC: 2008.1 - 2008.12	-6.212	-4.017	2.195
			(1.32)
Post-GFC: 2009.1 - 2012.5	-1.294	0.344	1.639
			(1.63)
Regulation: 2012.6 - 2019.12	-4.053	5.630	9.684***
			(9.43)
COVID: 2020.1 - 2020.12	1.891	23.601	21.710***
			(8.38)
Difference:			
COVID vs. Pre-GFC	-0.542	20.662***	
	(-0.41)	(10.52)	

Notes: This table presents the average trade imbalance of investment grade and high-yield bonds. Trade imbalances are measured according to Equation 8 and then averaged across dealers. T-statistics based on Driscoll and Kraay (1998) type of standard errors are presented in parentheses. *** (**) [*] denotes statistical significance at 1% (5%) [10%] level.

Table 4: Resiliency: Regulated vs. Non-regulated Dealers

	2008 GFC	2020 COVID	COVID - GFC
	(1)	(2)	(3)
Regulated Dealers			
β_5	4.452***	0.907	-3.545**
	(3.40)	(1.50)	(-2.46)
Half-Life	3.620***	1.323***	2.758**
	(3.84)	(19.21)	(2.43)
Non-Regulated Dealers			
β_5	3.590***	2.426**	-1.164
	(4.06)	(2.22)	(-0.83)
Half-Life	3.732***	2.295***	1.437
	(4.10)	(4.78)	(1.40)

Notes: This table presents the 5-week cumulative credit spread response (β^5) and shock half-life from Regression 9 for bonds primarily traded by regulated vs. non-regulated dealers during the 2008 GFC and 2020 COVID crises. T-statistics based on Driscoll and Kraay (1998) type of standard errors are presented in parentheses. *** (**) [*] denotes statistical significance at 1% (5%) [10%] level.

Table 5: Market Participant Response to Bond Downgrades

	Mutual Fund	Dealer (Pre-2008)	Dealer (Post-2012)
Dependent Variable:	Δ(Holding)	Imbalance	Imbalance
Panel A: Response to Downgrades			
Downgrade	-0.029***	-0.002	0.018***
	(-6.11)	(0.90)	(3.57)
Bond Controls	Y	Y	Y
Time Fixed Effects	Y	Y	Y
Observations	455,651	48,738	149,549
Within R-squared	0.006	0.003	0.005
Panel B: Response to Fallen Angels			
Fallen Angel	-0.060***	0.008	0.036**
	(-3.30)	(0.35)	(2.50)
Bond Controls	Y	Y	Y
Time Fixed Effects	Y	Y	Y
Observations	455,651	48,738	149,549
Within R-squared	0.006	0.003	0.005

Notes: This table presents the response of mutual fund and dealer positions to bond downgrades and fallen angel events from Regression 10. Standard errors are clustered at the bond level. *** (**) [*] denotes statistical significance at 1% (5%) [10%] level.

Table 6: Model Calibration and Validation

Panel A: Calibrated Parameters			
Parameter	Description	Value	Target Moment / Source
Resilience Parameters			
$\lambda^C = \lambda_0 + \lambda_1(\bar{I} - I)$			
λ_0	Baseline recovery rate	1.70	Half-life of 21.2 weeks (Table 1, pre-GFC)
λ_1	Spare capacity efficacy	4.44	Half-life of 6.9 weeks (Table 1, post-GFC)
λ^N	Crisis arrival rate	0.12	Avg. 8.25 years between crises (1987-2020)
Trading Frictions			
$\alpha(I)$	Trading speed function	$250 \cdot I$	1 day pre-GFC vs 5 day post-GFC (Wu 2020)
$\delta\pi_L$	Illiquidity shock arrival	0.33	Average Turnover (Feldhütter 2012)
η	Dealer bargaining power	0.9	Feldhütter (2012)

Panel B: Model Validation (Untargeted Moments)		
Moment	Model	Data
Liquidity Premium in Normal Times		
Pre-GFC ($I = \bar{I}$)	7 bps	$\approx$ 6-10 bps (Wu 2020)
Post-GFC ($I = 0.2\bar{I}$)	24 bps	$\approx$ 23 bps (Wu 2020)
Price Crash in Crisis		
Pre-GFC ($I = \bar{I}$)	5.6%	0.4% Yield Increase with 10-year duration (GFC)
Post-GFC ($I = 0.2\bar{I}$)	1.9%	0.17% Yield increase with 10-year duration (COVID)

Notes: This table outlines the calibration of the OTC model. Panel A lists the parameters set to match specific empirical targets. The resilience parameters (λ_0, λ_1) are calibrated to match the shock half-lives from our empirical analysis in Table 1 for the pre- and post-GFC periods, respectively. Panel B validates the model by showing its predictions for key moments that are not directly targeted. The model is evaluated in two regimes: a "pre-GFC" high-inventory regime ($I = 100\%\bar{I}$) and a "post-GFC" low-inventory regime ($I = 20\%\bar{I}$). $r = 0.1$ to match the average duration of 10 years, $\epsilon_H = 10$, $\epsilon_L = 4$.

Table 7: Counterfactual: The Role of Regulation in the Fed's COVID-19 Intervention

	Recovery Speed (λ)	Half-Life (weeks)	Price Crash (%)
Panel A: Empirical Estimation of Fed Intervention Effect (λ_{Fed})			
COVID Pre-Fed (2019.1-2020.3)	5.39	6.68	-
COVID Post-Fed (2020.4-2021.6)	7.50	4.80	-
Implied Fed Effect (λ_{Fed})	2.11	-	-
Panel B: Model Counterfactual			
Scenario 1: Actual (Post-GFC Reg + Fed)			
Regulatory Capacity ($\lambda_0 + \lambda_1(\bar{I} - I)$)	5.25	6.87	
Total with Fed (λ_{total})	7.36	4.90	-1.35%
Scenario 2: Counterfactual (Pre-GFC + Fed)			
Regulatory Capacity (λ_0)	1.70	21.24	
Total with Fed (λ_{total})	3.81	9.46	-2.56%
Difference (Actual - Counterfactual)	+3.55	-4.56 weeks	+1.21%

Notes: This table presents a counterfactual analysis on the effectiveness of the Federal Reserve's 2020 intervention under different regulatory regimes. Panel A empirically estimates the marginal impact of the Fed's intervention (λ_{Fed}). We run the local projection (3) on two sub-periods nested together: January 2019 - March 20th, 2020 and March 20th, 2020 - June 2021. The recovery speed λ is annualized and calculated from the estimated shock half-life as $\lambda = (\ln(2)/\text{Half-Life}) \times 52$. The difference in λ between the two periods is our estimate of λ_{Fed}. Panel B simulates two scenarios using the calibrated model from Table 6. In both scenarios, the market is hit by the COVID shock and the Fed intervenes with force $\lambda_{Fed} = 2.11$. *Scenario 1 (Actual)* assumes the post-GFC low-inventory regime ($I = 0.2\bar{I}$), resulting in high dealer spare capacity and a high underlying recovery speed. *Scenario 2 (Counterfactual)* assumes a pre-GFC high-inventory regime ($I = \bar{I}$), resulting in zero spare capacity and a low underlying recovery speed. The "Price Crash" is the model-implied maximum price drop $(p^C - p^N)/p^N$.

APPENDIX

B Appendix

B.1 Micro-Foundation 1 of OTC Model in Section 2: Dealer Capacity

This microfoundation follows Weill (2007). In the model, there are three types of agents: buyers (B), owners (O) and sellers (S). Buyers and owners have high valuations of the bond. There is a liquidity shock that happens at the Poisson rate of κ, upon which the owner of the bond wants to sell it, and the buyer of the bond leaves the market. Trades happen when buyers and sellers meet at the Poisson rate of λ. Finally, buyers enter the market with some amount $I(t)$ each time. In this model we take the perspective of a potential seller. This is a natural assumption as during distress, a seller typically suffers more from illiquidity when they cannot find potential buyers. Naturally, one could interpret the buyer agent (B) as the dealer of the market and $I(t)$ as the amount of capital they commit to trading. As before, we assume that there is a maximum capital capacity $I(t) < \bar{I}$. In the model, we assume that capital $I(t)$ is controlled by regulators and therefore abstract from individual dealer maximization problems. The agents distributions therefore satisfy the following:

$$\begin{aligned} \dot{u_B} &= -\lambda u_B u_S - \kappa u_B + I(t) \\ \dot{u_S} &= -\lambda u_B u_S + \kappa u_O \\ \dot{u_O} &= \lambda u_B u_S - \kappa u_O \end{aligned} \tag{14}$$

Finally, total bond supply is s and market clears: $u_S + u_O = s$. These equations are intuitive. Each time a buyer enters the market with some capital $I(t) < \bar{I}$. He trades with a seller at rate λ, upon which he becomes an owner of the bond and leaves the market if this buyer is hit by a liquidity shock at rate κ. And finally, the owner wants to sell the bond when he is hit by a liquidity shock at the rate of κ.

In normal times there is no disruption which means the model is in the steady state.

$$\begin{aligned} 0 &= -\lambda u_B u_S - \kappa u_B + I \\ 0 &= -\lambda u_B u_S + \kappa u_O \\ 0 &= \lambda u_B u_S - \kappa u_O \end{aligned} \tag{15}$$

One can show that in this case, more stringent capital requirements imply a longer trading delay. More formally, when the model is in the steady state, a lower capital commitment, $I \downarrow$ means that sellers face longer trading delays and have to wait longer to sell the asset: $\frac{1}{\lambda u_B} \uparrow$. A formal proof of this claim can be found in Afonso (2011).

However, the above analysis is only one side of the argument. The design of regulations is to prevent large disruptions of the market. Therefore, it is important that we look beyond the steady state of the model and study the transition dynamics when there is an aggregate liquidity shock. Specifically, suppose the aggregate shock hits the population all at once (at time 0). Buyers and owners are all destroyed and the entire assets are in the hands of sellers ($u_S(0) = s$). It is precisely this moment when additional capital $\bar{I} - I$ can be used to accommodate additional selling pressures:

$$\begin{aligned} \dot{u_B} &= -\lambda u_B u_S - k u_B + f_t(\bar{I} - I) + (1 - e^{-\hat{k}t})I \\ \dot{u_S} &= -\lambda u_B u_S + k u_O \\ \dot{u_O} &= \lambda u_B u_S - k u_O, \end{aligned} \tag{16}$$

where $f(0) = 0$, $f' > 0$, $f_\infty = 0$. Specifically, $(1 - e^{-\hat{k}t})I$ represents capital destruction upon the aggregate shock. $f(\bar{I} - I)$ represents the additional capital that can be brought to restore the market. In other words, this is the amount of capital dealers can use to "lean against the wind" during market crashes. If dealers use too much capital during normal times $I \approx \bar{I}$, then there is no additional capital that dealers can commit in a crisis. The benefit of additional capital$\bar{I} - I$ during the crisis is that it can stabilize the buyers or liquidity providers (u_B). If buyers have enough capacity $I << \bar{I}$, then it is possible that $f_t(\bar{I} - I)$ can make $\dot{u_B} = 0$ even after the aggregate shock hits.

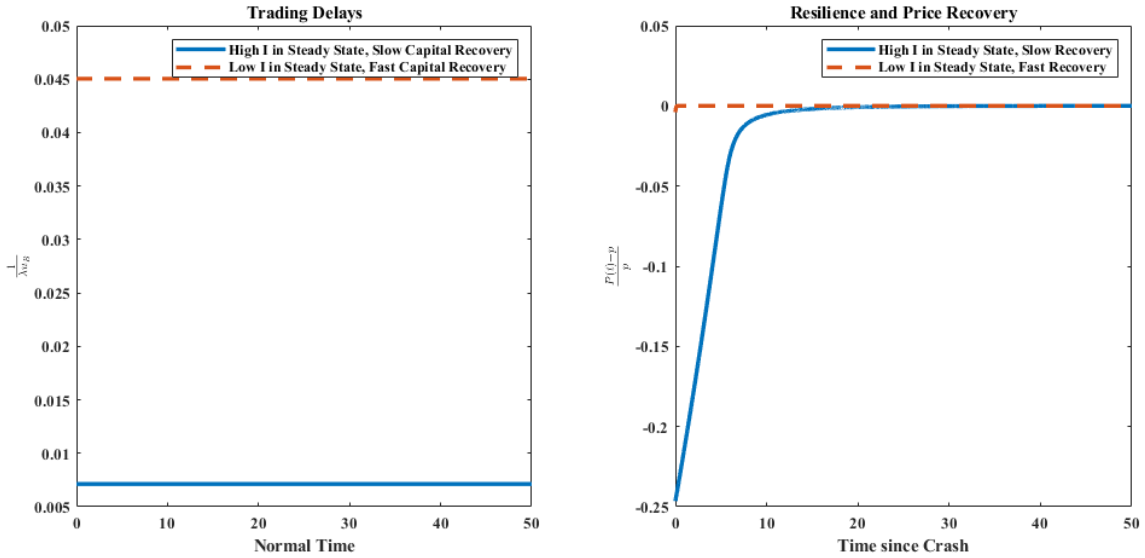
Finally, the evolution of asset prices comes from the following:

$$\begin{aligned} \dot{V_B} &= rV_B - \lambda u_S(V_O - p - V_B) - k(0 - V_B) \\ \dot{V_S} &= rV_S - \lambda u_B(p - V_S) \\ \dot{V_O} &= rV_O - k(V_S - V_O) \end{aligned} \tag{17}$$

where price p is determined through the Nash bargaining: $p = (1 - \eta)(V_O - V_B) + \eta V_S$ and η is

buyer's bargaining power. These functions are intuitive. A bond buyer (B) meets a seller at the rate λu_S, upon which he buys the bond at the price p and becomes an owner (O). A buyer (B) can also exit the market if he is hit by a liquidity shock at the rate κ. Similarly, a seller (S) meets a buyer (B) at the rate λu_B, upon which the seller sells the bond at the price p and exits the market. Finally, an owner (O) becomes a low valuation seller (S) when he is hit by a liquidity shock at the rate κ. Figure A1 shows how the price will recover when dealers have more capital to "lean against with wind" during time of the crisis $(\bar{I} - I)$, at the cost of longer trading delays in normal times.

Figure A1: Immediacy vs. Resiliency



The left panel shows the average trading delays (immediacy) in the high inventory (blue solid) vs. low inventory (red dashed) regimes. The right panel shows the price recovery (resiliency) in the high inventory (blue solid) vs. low inventory (red dashed) regimes.

B.2 Micro-Foundation 2 of OTC Model in Section 2: VaR Constraint

The second microfoundation follows Gârleanu and Pedersen (2007) who explicitly model the value-at-risk constraint. Suppose the asset fundamental follows a stochastic process

$$dX_t = \sigma_X dW_t$$

where σ_X is the volatility. It has a price $P(X)$ which will be determined in equilibrium.

The distribution of agents follows Duffie, Gârleanu, and Pedersen (2005). In addition, suppose

the owners (ho and lo) hold $\bar{\theta}$ unit of assets. The distributions should sum to 1 and the market should clear:

$$\begin{aligned}
\dot{\mu}_{lo}(t) &= -2\lambda\mu_{hn}(t)\mu_{lo}(t) - \lambda_u\mu_{lo}(t) + \lambda_d\mu_{ho}(t) \\
\dot{\mu}_{hn}(t) &= -2\lambda\mu_{hn}(t)\mu_{lo}(t) - \lambda_d\mu_{hn}(t) + \lambda_u\mu_{ln}(t) \\
\dot{\mu}_{ho}(t) &= 2\lambda\mu_{hn}(t)\mu_{lo}(t) - \lambda_d\mu_{ho}(t) + \lambda_u\mu_{lo}(t) \\
\dot{\mu}_{ln}(t) &= 2\lambda\mu_{hn}(t)\mu_{lo}(t) - \lambda_u\mu_{ln}(t) + \lambda_d\mu_{hn}(t) \\
1 &= \mu_{ho} + \mu_{hn} + \mu_{lo} + \mu_{ln} \\
\Theta &= \bar{\theta}(\mu_{ho} + \mu_{lo})
\end{aligned} \tag{18}$$

where Θ is the total supply of the asset, h and l indicate whether the agent is of a high or low valuation of the asset, and o and n indicate whether the agent currently owns the asset or not. λ is the matching intensity, λ_u (λ_d) is the intensity that low (high) valuation agents become high (low) valuation agents. Again, we take the perspective of a potential seller, so we are interested in the expected time to sell an asset, as well as the measure of the potential buyers μ_{hn}, which one can interpret as the measure of liquidity providers or dealers.

Following Gârleanu and Pedersen (2007), guess the value functions and price have the form $V_\xi(X,t) = \bar{\theta}\frac{X}{r}\mathbb{1}_{\xi\in\{ho,lo\}} + \bar{\theta}v_\xi(t)$, and $P(X,t) = \frac{X}{r} + p(t)$, where v_ξ and p satisfy the following:

$$\begin{aligned}
\dot{v}_{lo}(t) &= rv_{lo}(t) - \lambda_u(v_{ho}(t) - v_{lo}(t)) - 2\lambda\mu_{hn}(t)(p(t) + v_{ln}(t) - v_{lo}(t)) + \delta \\
\dot{v}_{ln}(t) &= rv_{ln}(t) - \lambda_u(v_{hn}(t) - v_{ln}(t)) \\
\dot{v}_{ho}(t) &= rv_{ho}(t) - \lambda_d(v_{lo}(t) - v_{ho}(t)) \\
\dot{v}_{hn}(t) &= rv_{hn}(t) - \lambda_d(v_{ln}(t) - v_{hn}(t)) - 2\lambda\mu_{lo}(t)(v_{ho}(t) - v_{hn}(t) - p(t)) \\
p(t) &= (v_{lo}(t) - v_{ln}(t))(1-q) + (v_{ho}(t) - v_{hn}(t))q
\end{aligned} \tag{19}$$

and q is the bargaining power and δ is the holding costs for lo type investors.

Finally, we determine asset holdings $\bar{\theta}$ through a VaR-type of constraint:

$$\frac{1}{dt}var_t[\bar{\theta}dP_t(X)] \leq \bar{\sigma}^2$$

where $\bar{\theta}$ is the agent risk limit. Since $P(X,t) = \frac{X}{r} + p(t)$, the asset holding satisfies:

$$\bar{\theta} = \frac{\bar{\sigma} \times r}{\sigma_X}. \tag{20}$$

Now consider a stressed period when asset volatility goes up to the GFC level, $\sigma_X \uparrow \sigma_{GFC}$, the VaR constraint dictates that the asset holding will immediately go down $\bar{\theta} \downarrow$. One can show from equation (18) that μ_{hn} will immediately plummet, and μ_{lo} will immediately increase. This volatility spike is therefore akin to an aggregate preference shock in Duffie, Gârleanu, and Pedersen (2007) and Weill (2007), with a sudden increase in potential sellers. The asset price will rebound slowly as measures of potential buyers μ_{hn} gradually recovers from stress.

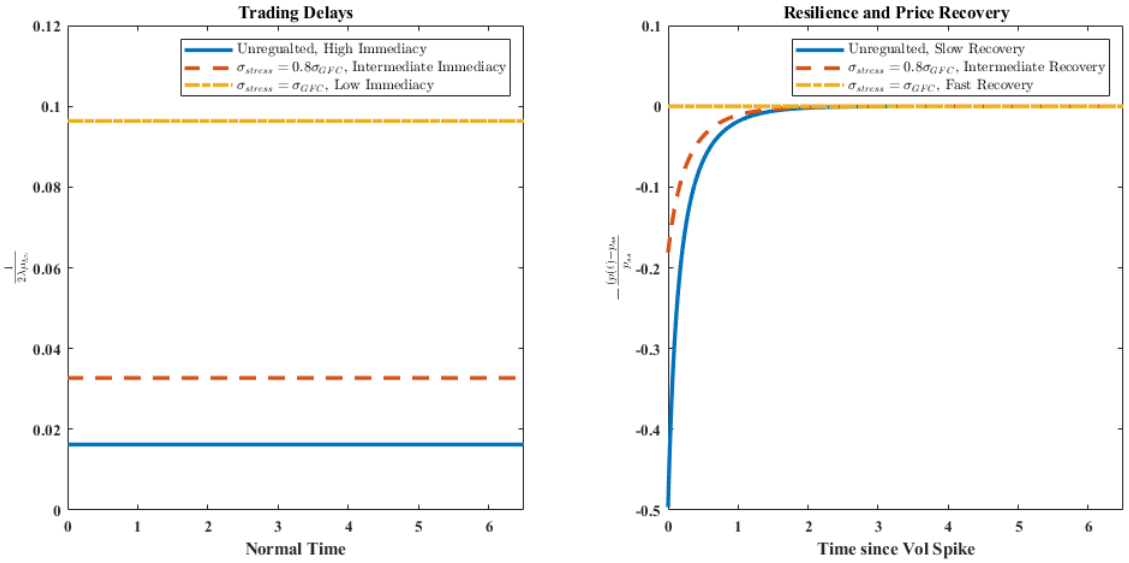
Now consider the impact of regulations. Instead of using the current volatility of the fundamental as the input of the VaR constraint, regulations such as Basel II.5 impose a stressed VaR (SVAR) constraint and so the heightened volatility value in stress times σ_{stress} should be the input to the VaR constraint even in normal times:

$$\bar{\theta}_{reg} = \frac{\bar{\sigma} \times r}{\sigma_{stress}} \tag{21}$$

Since $\bar{\theta}_{reg} < \bar{\theta}$, μ_{hn} is always lower in steady states under the regulated economy, and so trading delays $\frac{1}{\lambda \mu_{hn}}$, the expected time to sell in normal times, are always higher with regulation. However, the gain from regulation is that the measure of liquidity providers, μ_{hn}, will become more stable and less prone to collapse driven by market volatility. In fact, μ_{hn} will only collapse if volatility shoots up above σ_{stress}. This will make the whole economy recover faster and the price crash less severe.

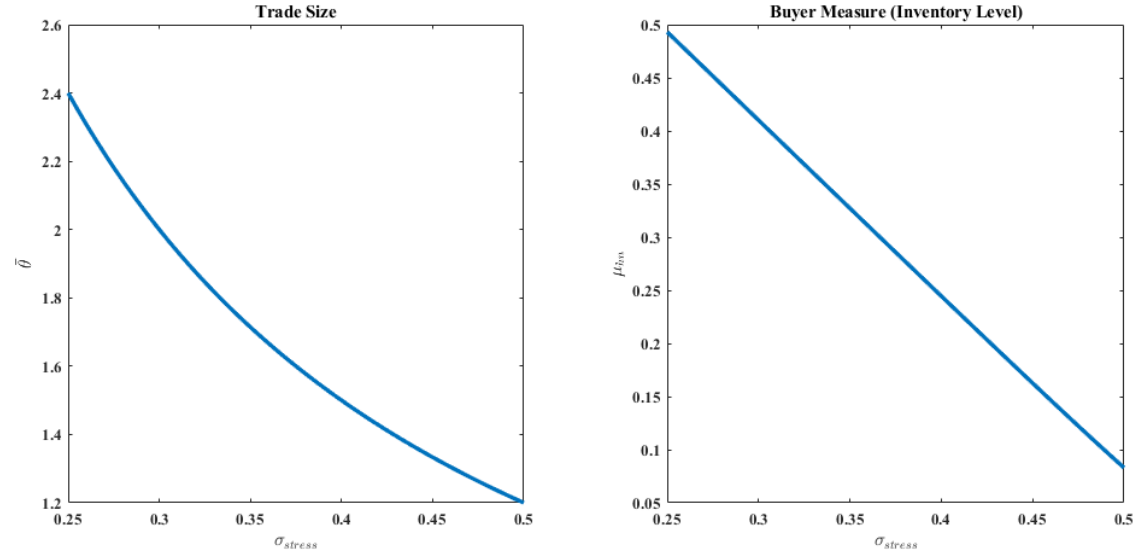
In Figure A2 I plot the average expected time to sell $\frac{1}{2\lambda \mu_{hn}}$ in normal times, and the price recovery $-\frac{p(t)-p_{ss}}{p_{ss}}$ when the economy is unregulated with a regular VaR (blue solid) vs. medium SVaR $\sigma_{stress} = 0.8\sigma_{GFC}$ (red dashed) vs. highly regulated SVaR $\sigma_{stress} = \sigma_{GFC}$ (yellow dot), where σ_{GFC} is the crisis time volatility at time 0. In Figure A3, I plot the level of trade size and dealer inventory (μ_{hn}) in steady states as a function of regulation parameter σ_{stress}.

Figure A2: Immediacy vs. Resiliency



Notes: The left panel shows the average trading delays (immediacy) in the unregulated economy with regular VaR (blue solid) vs. medium-level SVaR $\sigma_{stress} = 0.8\sigma_{GFC}$ (red dashed) vs. highly regulated SVaR $\sigma_{stress} = \sigma_{GFC}$ (yellow dot). The right panel shows the price recovery (resiliency) in the unregulated economy with regular VaR (blue solid) vs. medium-level SVaR $\sigma_{stress} = 0.8\sigma_{GFC}$ (red dashed) vs. highly regulated SVaR $\sigma_{stress} = \sigma_{GFC}$ (yellow dot). Parameter values are from Duffie, Gârleanu, and Pedersen (2007) and Gârleanu and Pedersen (2007): $r = 0.1$, $\lambda = 125$, $\lambda_d = 0.2$, $\lambda_u = 2$, $\delta = 3$, $q = 0.5$, $\Theta = 1$, $\bar{\sigma} = 6$, $\sigma_X = 0.25$, $\sigma_{GFC} = 0.5$.

Figure A3: Trade Size and Inventory Level in Steady States



Notes: The left panel shows the level of trade size $\bar{\theta}$ in steady states as a function of σ_{stress}. The right panel shows the level of inventory μ_{hn} in steady states as a function of σ_{stress}. Parameter values are from Duffie, Gârleanu, and Pedersen (2007) and Gârleanu and Pedersen (2007): $r = 0.1$, $\lambda = 125$, $\lambda_d = 0.2$, $\lambda_u = 2$, $\delta = 3$, $q = 0.5$, $\Theta = 1$, $\bar{\sigma} = 6$.

B.3 Proof of Proposition 1

We will show the following:

1) $p^N - p^C$ and $\frac{p^N - p^C}{p^N}$ are both decreasing in the recovery speed λ^C.

2) $p^N - p^C$ is increasing in the trading speed κ.

Proof. We know the prices are equal to:

$$p^N = \frac{\bar{\epsilon}_H^N}{r} - \frac{\kappa\lambda^N}{r(r+\kappa)(r+\lambda^C+\lambda^N)}(\bar{\epsilon}_H^N - \bar{\epsilon}_H^C)$$
$$p^C = \frac{\bar{\epsilon}_H^C}{r} - \frac{\kappa\lambda^C}{r(r+\kappa)(r+\lambda^C+\lambda^N)}(\bar{\epsilon}_H^C - \bar{\epsilon}_H^N)$$

Subtracting the second equation from the first gives:

$$\begin{aligned}
p^N - p^C &= \left(\frac{\bar{\epsilon}_H^N}{r} - \frac{\bar{\epsilon}_H^C}{r}\right) - \left[\frac{\kappa\lambda^N(\bar{\epsilon}_H^N - \bar{\epsilon}_H^C)}{r(r+\kappa)(r+\lambda^C+\lambda^N)} - \frac{\kappa\lambda^C(\bar{\epsilon}_H^C - \bar{\epsilon}_H^N)}{r(r+\kappa)(r+\lambda^C+\lambda^N)}\right] \\
&= \frac{\bar{\epsilon}_H^N - \bar{\epsilon}_H^C}{r} - \left[\frac{\kappa\lambda^N(\bar{\epsilon}_H^N - \bar{\epsilon}_H^C) + \kappa\lambda^C(\bar{\epsilon}_H^N - \bar{\epsilon}_H^C)}{r(r+\kappa)(r+\lambda^C+\lambda^N)}\right] \\
&= (\bar{\epsilon}_H^N - \bar{\epsilon}_H^C)\left[\frac{1}{r} - \frac{\kappa(\lambda^N+\lambda^C)}{r(r+\kappa)(r+\lambda^C+\lambda^N)}\right] \\
&= (\bar{\epsilon}_H^N - \bar{\epsilon}_H^C)\left[\frac{r+\kappa+\lambda^N+\lambda^C}{(r+\kappa)(r+\lambda^N+\lambda^C)}\right]
\end{aligned}$$

One can show that:

$$\bar{\epsilon}_H^N - \bar{\epsilon}_H^C = (r+\kappa)(z^N - z^C)\left[\frac{\bar{\epsilon}}{r+\kappa+\lambda^N+\lambda^C} + \frac{\epsilon_H - \bar{\epsilon}}{r+\kappa+\delta+\lambda^N+\lambda^C}\right]. \tag{22}$$

This implies that the absolute price crash is:

$$p^N - p^C = (z^N - z^C)\left[\frac{\bar{\epsilon}}{r+\kappa+\lambda^N+\lambda^C} + \frac{\epsilon_H - \bar{\epsilon}}{r+\kappa+\delta+\lambda^N+\lambda^C}\right]\left(\frac{r+\kappa+\lambda^N+\lambda^C}{r+\lambda^N+\lambda^C}\right) \tag{23}$$

Therefore the absolute price crash $p^N - p^C$ is decreasing in λ^C, and is increasing in κ.

In addition, we know $p^N = \frac{\bar{\epsilon}_H^N}{r} - \frac{\kappa\lambda^N}{r(r+\kappa)(r+\lambda^C+\lambda^N)}(\bar{\epsilon}_H^N - \bar{\epsilon}_H^C)$. Notice that

$$\bar{\epsilon}_H^N = \frac{(r+\kappa+\lambda^C)z^N + \lambda^N z^C}{r+\kappa+\lambda^C+\lambda^N}\bar{\epsilon} + \frac{r+\kappa}{r+\kappa+\delta}\frac{(r+\kappa+\delta+\lambda^C)z^N + \lambda^N z^C}{r+\kappa+\delta+\lambda^C+\lambda^N}(\epsilon_H - \bar{\epsilon})$$

is increasing in λ^C because $z^N > z^C$ and $\epsilon_H > \bar{\epsilon}$. Also, $\frac{\kappa\lambda^N}{r(r+\kappa)(r+\lambda^C+\lambda^N)}$ is decreasing in λ^C, and $(\bar{\epsilon}_H^N - \bar{\epsilon}_H^C)$ is decreasing in λ^C according to Equation (22). Taken together, this means p^N is increasing in λ^C. Since $p^N - p^C$ is decreasing in λ^C, and p^N is increasing in λ^C, this means that the relative price crash $\frac{p^N - p^C}{p^N}$ is also decreasing in λ^C.

□

B.4 Proof of Proposition 2

Proof. As Equation (23) shows, we have:

$$p^N - p^C = (z^N - z^C)\left[\frac{\bar{\epsilon}}{r+\kappa+\lambda^N+\lambda^C} + \frac{\epsilon_H - \bar{\epsilon}}{r+\kappa+\delta+\lambda^N+\lambda^C}\right]\left(\frac{r+\kappa+\lambda^N+\lambda^C}{r+\lambda^N+\lambda^C}\right)$$

Since $\kappa >> r$, or λ^N, or λ^C under reasonable calibration exercises,[9] we have:

$$p^N - p^C \approx (z^N - z^C)\left[\frac{\epsilon_H}{r+\lambda^N+\lambda^C}\right].$$

This means that the elasticity with respect to the recovery speed is approximately:

$$\frac{\partial(p^N - p^C)}{\partial\lambda^C}\frac{\lambda^C}{p^N - p^C} \approx -\frac{\lambda^C}{r+\lambda^N+\lambda^C}, \tag{24}$$

which is approximately -1. So one percent increase in λ^C is almost entirely translated to one percent decrease in $p^N - p^C$.

Finally, rewrite Equation (23) as

$$p^N - p^C = (z^N - z^C)\frac{\bar{\epsilon}}{r+\lambda^N+\lambda^C} + (z^N - z^C)\frac{\epsilon_H - \bar{\epsilon}}{r+\lambda^N+\lambda^C}\frac{r+\kappa+\lambda^N+\lambda^C}{r+\kappa+\delta+\lambda^N+\lambda^C}.$$

[9] If trading delays are five days, then $\kappa = 50$

Straightforward calculations show that the elasticity with respect to the trading speed is equal to:

$$\frac{\partial(p^N - p^C)}{\partial \kappa} \frac{\kappa}{p^N - p^C} = \frac{\kappa\delta(\epsilon_H - \bar{\epsilon})}{[r + \kappa + \delta + \lambda^N + \lambda^C][\epsilon_H(r + \kappa + \lambda^N + \lambda^C) + \bar{\epsilon}\delta]}, \tag{25}$$

which is of the order of magnitude of $\mathcal{O}(\kappa^{-1})$, as κ is a lot larger than other parameters under realistic calibration.

□

B.5 State Dependent Trading Intensities

In the baseline model in Section 2, customers meet dealers at a constant Poisson rate α, regardless of the aggregate state. This section extends the model to allow the search (meeting) intensity to depend on the aggregate state. In particular, let

$$\alpha^N \quad \geq \quad \alpha^C$$

denote the meeting rates in the Normal state N and the Crisis state C, respectively. This extension captures the idea that trading intensity (immediacy) can deteriorate in a crisis, while still preserving the tractability of the baseline model.

With state-dependent search, equation (1) becomes

$$rV_i^s(a) = z^s\epsilon_i a + \lambda^s\big(V_i^{s'}(a) - V_i^s(a)\big) + \delta \sum_{j\in\{H,L\}} \pi_j\big(V_j^s(a) - V_i^s(a)\big) + \alpha^s(1-\eta)\Big(V_i^s(a_i^s) - V_i^s(a) - p^s(a_i^s - a)\Big), \tag{26}$$

where α^s is the meeting rate in aggregate state s.

As in the main text, in a stochastic stationary equilibrium, the value function is linear in a, and the optimization pins down the desired holdings a_i^s and a shadow marginal value ξ^s in each aggregate state s. Intuitively, ξ^s is the value to a marginal (high-type) investor of holding one additional unit of the bond in state s.

Solving the HJB system (26) yields a pair of linear equations linking the shadow values ξ^N and

ξ^C to the prices p^N and p^C:

$$\xi^N = rp^N - c^N\big(p^C - p^N\big), \qquad \xi^C = rp^C - c^C\big(p^N - p^C\big), \tag{27}$$

where

$$c^s \;:=\; \frac{\kappa^s \lambda^s}{r + \kappa^s + \lambda^N + \lambda^C}, \qquad \kappa^s := \alpha^s(1-\eta), \quad s \in \{N, C\}.$$

The term c_s summarizes how strongly a change in the aggregate state matters between meetings in state s. trading speed κ^s and in the transition intensity λ_s.

The shadow values (ξ^N, ξ^C) themselves are determined, as in the baseline model, by the expected discounted flow payoff until the next meeting. For example, for the high-valuation type H,

$$\xi^s = \bar{\epsilon}^s_H = (r + \kappa^s)\,\mathbb{E}\left[\int_0^T e^{-rt} z^{S_t}\, \epsilon_{I_t}\, dt \;\middle|\; S_0 = s, I_0 = H\right], \tag{28}$$

where T is the (state-dependent) time of the next meeting and S_t and I_t denote the aggregate and idiosyncratic states between trades.

Equations (27) form a 2×2 linear system in (p^N, p^C), which can be solved explicitly. The resulting pricing formulas are

$$p^N = \frac{1}{r}\frac{(r + c^C)\,\xi^N + c^N\,\xi^C}{(r + c^N + c^C)}, \qquad p^C = \frac{1}{r}\frac{(r + c^N)\,\xi^C + c^C\,\xi^N}{(r + c^N + c^C)}. \tag{29}$$

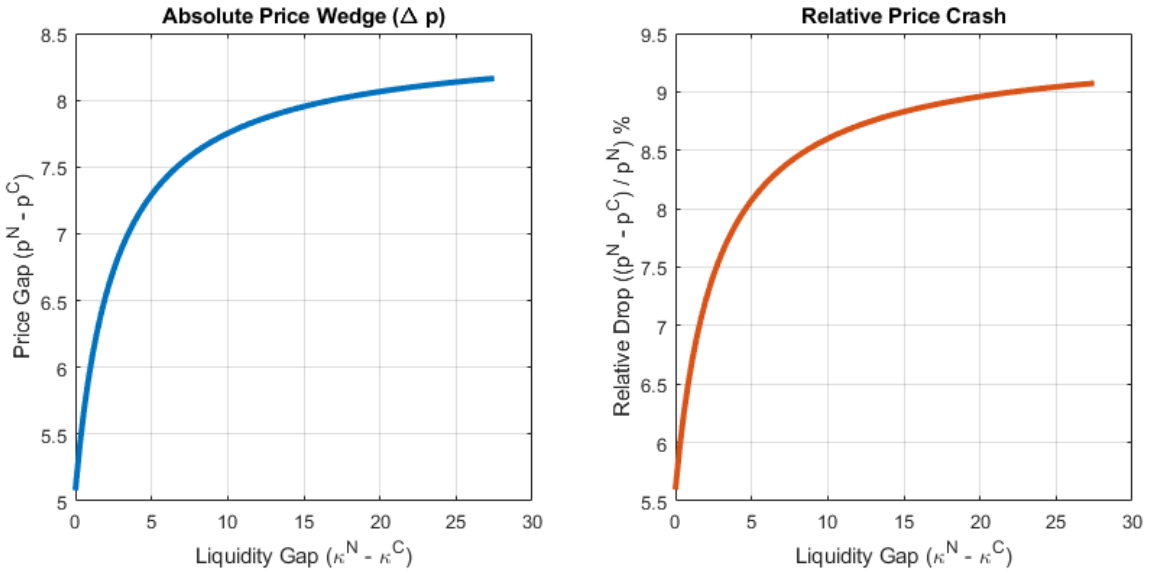
The price gap between the Normal and Crisis states is

$$p^N - p^C = \frac{\xi^N - \xi^C}{r + c^N + c^C}. \tag{30}$$

One can show that the price gap $p^N - p^C$ becomes smaller when the trading friction gap $|\kappa^N - \kappa^C|$ is reduced, as can be seen from Figure A4. In the context of regulation, a reduction in normal-time search intensity κ^N (worse immediacy) but a higher crisis floor κ^C (more stable intermediation in stress) thus leads to a a smaller price gap $p^N - p^C$. This captures the idea that better-capitalized dealers can keep trading from collapsing in crises, improving the *resiliency* of OTC market liquidity

even as they provide less immediacy in normal times.

Figure A4: Impact of Asymmetric Search Intensities on Market Resiliency



Notes: This figure how the price gap $p^N - p^C$ or $\frac{p^N - p^C}{p^N}$ decreases when the trading friction gap $\kappa^N - \kappa^C$ is reduced.

B.6 Robustness

We conduct a few robustness checks. First, we see whether the same improvement in resiliency shows up in the panel of bonds, I run the following panel regression with bond fixed effects:

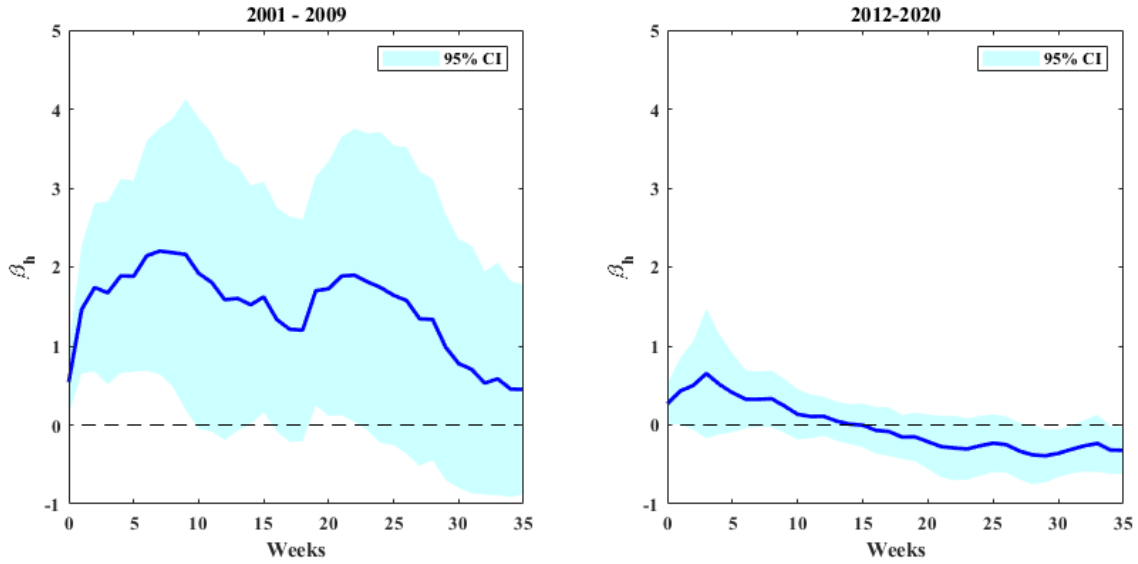
$$\textit{Credit-Yield}_{i,t+h} - \textit{Credit-Yield}_{i,t} = \alpha_i^h + \beta^h \times \Delta \log(VIX)_t + \textit{Lagged Credit-Yield} + \epsilon_{i,t+h}. \quad (31)$$

Figure A5 presents the results. We see that for a panel of bonds, the response to 1% increase in weekly VIX leads to almost 2% increase in the average bond yields in the pre-GFC period, while the average response is much more muted after the GFC.

We also add contemporaneous changes in the corporate CDS in the main regression 3 to isolate the pure liquidity shock from VIX. Figure A6 presents the results. The response of credit spread to the aggregate liquidity shock is similar to our baseline figure when we hold constant the contemporaneous shock to fundamental credit risk.

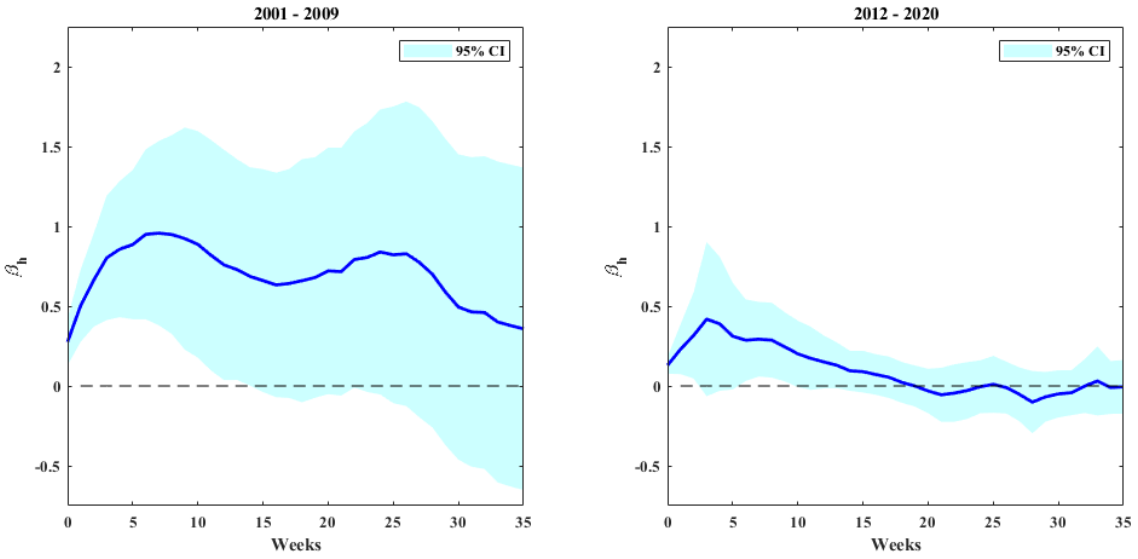
To obtain a more stable estimate of the mean-reversion rate in the yields, I run the following

Figure A5: Corporate Bond Resiliency: Panel Regression



Notes: This figure shows the β^h from Regression 31, as well as the 95% of the confidence intervals using the Driscoll and Kraay (1998) type of standard errors with bond fixed effect.

Figure A6: Corporate Bond Resiliency: Adding CDS controls



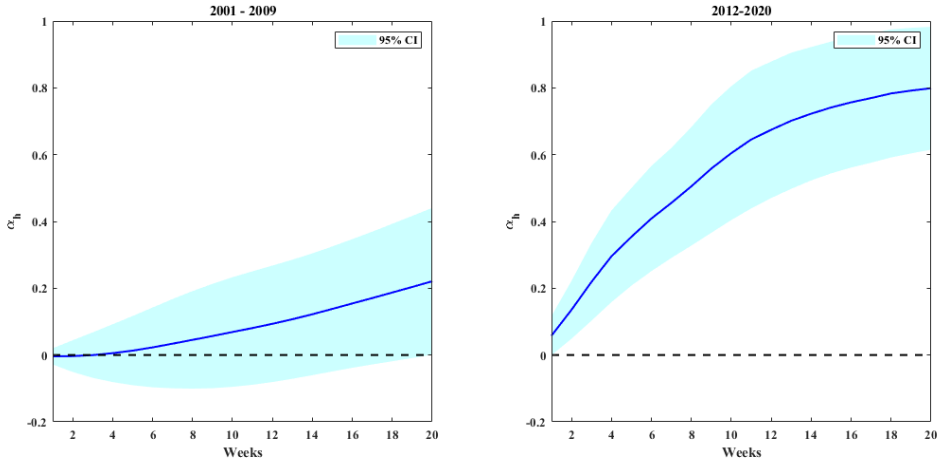
Notes: This figure shows the β^h from Regression 3 by adding the contemporaneous changes in the corporate CDS, as well as the 95% of the confidence intervals using the Driscoll and Kraay (1998) type of standard errors with bond fixed effect.

regression:

$$\textit{Credit-Spread}_{t+h} - \textit{Credit-Spread}_t = c^h + \alpha^h(-\textit{Credit-Spread}_t) + \epsilon_{t+h}. \tag{32}$$

We see that after the great financial crisis, the corporate bond market has become more resilient

Figure A7: Corporate Bond Resiliency: Alternative Measure II



Notes: This figure shows the α^h from Regression 32, as well as the 95% of the confidence intervals with Newey and West (1987) type of standard errors with bond fixed effect.

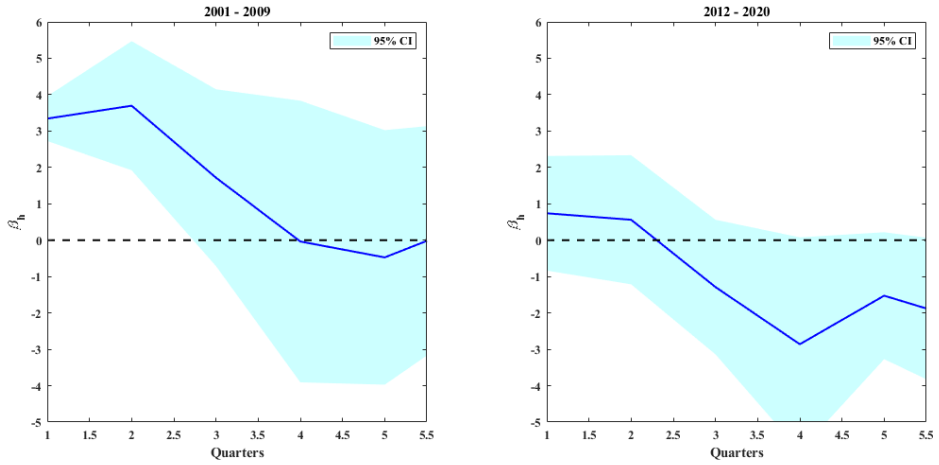
as the yields mean revert more quickly compared to the pre-GFC period.

Finally, to address the concern that VIX perhaps may not capture the sudden liquidity shock well, I use the corporate bond mutual fund flow-driven demand shocks (Lou 2012, Chaudhary, Fu, and Li 2022) and look at whether bond yields are able to absorb these demand shocks. Aggregate liquidity shocks trigger fund outflows which lead to price drops and subsequent recovery. I first construct the quarterly demand shocks at the bond level following Chaudhary, Fu, and Li (2022) and run the following panel regression:

$$\textit{Credit-Spread}_{i,t+h-1} - \textit{Credit-Spread}_{i,t-1} = c_i^h + \beta_h(-\text{DemandShock}_{i,t}) + \epsilon_{i,t+h}. \tag{33}$$

We see similar patterns of improved resiliency after the great financial crisis. Prior to the great financial crisis, it took more than 2 quarters for bond yields to fully absorb the liquidity shocks driven by demand, while such absorption happens much faster and the price impact disappears after the great financial crisis.

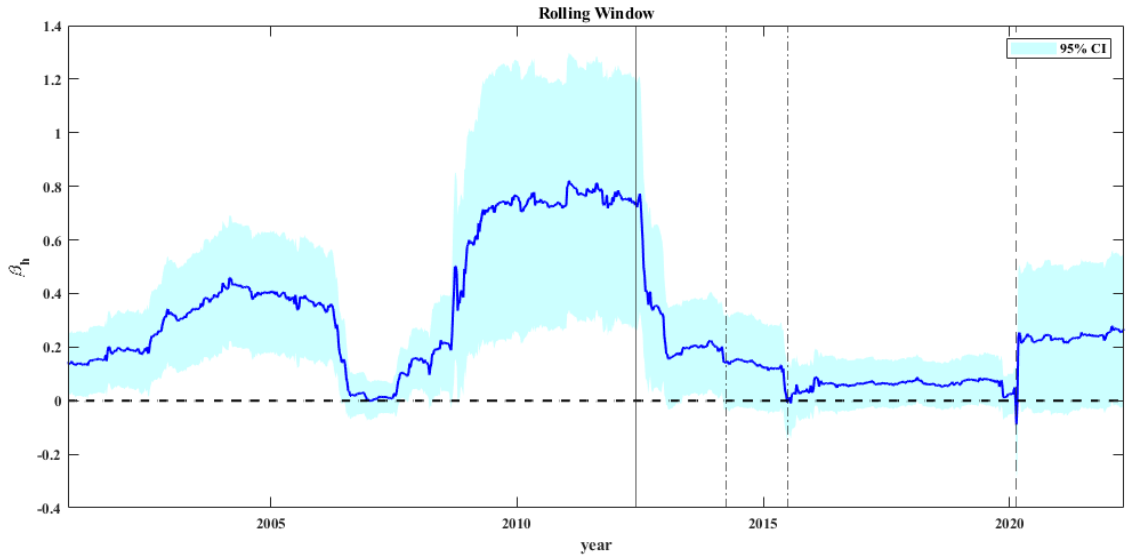
Figure A8: Corporate Bond Resiliency: Demand Shocks



Notes: This figure shows the β_h estimates from Regression 33. as well as the 95% of the confidence intervals with Driscoll and Kraay (1998) type of standard errors with bond fixed effect.

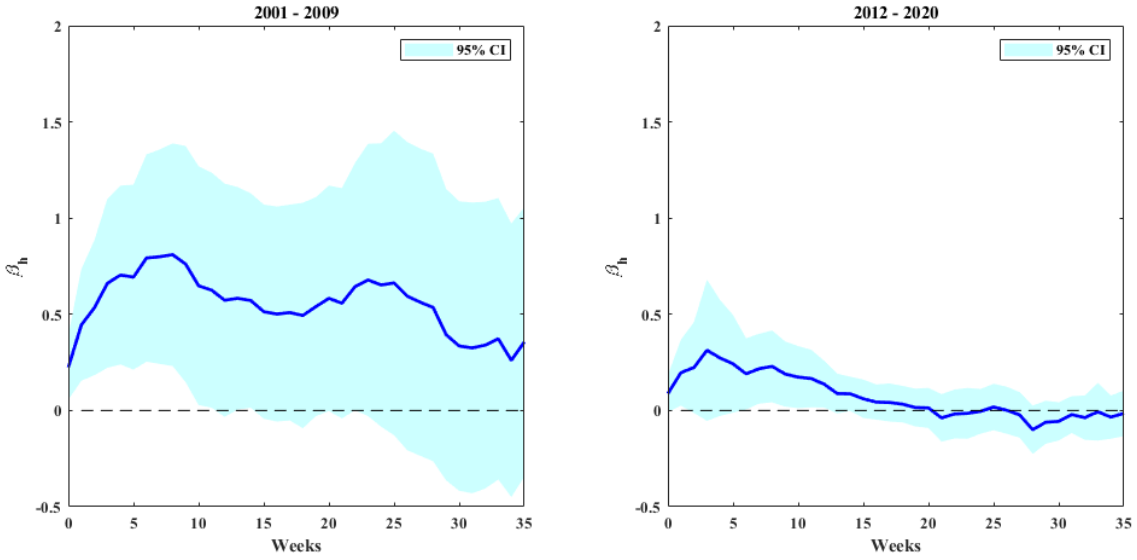
We also run Regression (3) on a rolling window basis. Figure A9 plots the time series of β^5. Finally, we conduct the time series analysis on the liquidity component of the credit spread by subtracting a high-yield CDS component.

Figure A9: Rolling Window



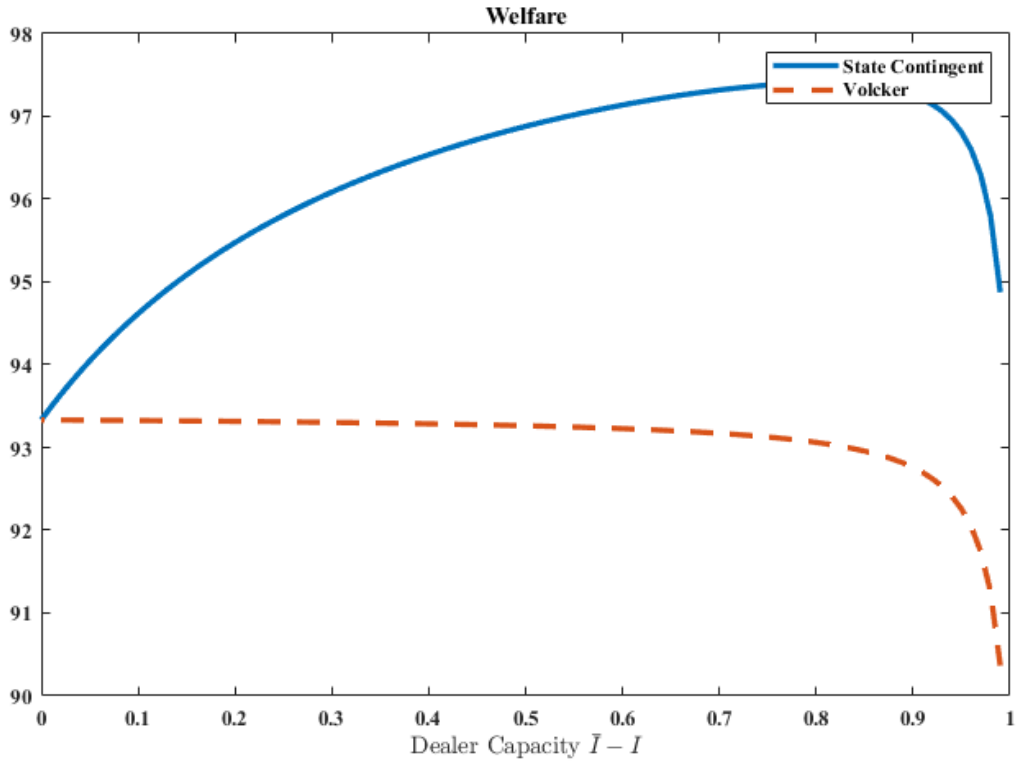
Notes: This figure plots β^5 from Regression (3) run on a rolling window basis. The dashed lines correspond to the implementation of the post-GFC regulations and the market crash due to COVID.

Figure A10: Liquidity Component



Notes: This figure plots the β^h from Regression (3). The dependent variable is the liquidity component of the credit spread by subtracting a high-yield CDS component.

Figure A11: Welfare



Notes: This figure plots welfare in equation (12) as a function of the dealer balance sheet capacity $\bar{I} - I$, for both the state-contingent recovery $\lambda^C(\bar{I} - I)$ as well as the draconian state-independent $\lambda^C(0)$.